Bulk and interfacial properties of polar and molecular fluids

Peter Frodl and S. Dietrich
Fachbereich Physik, Bergische Universität Wuppertal, Postfach 100127, D-5600 Wuppertal 1, Federal Republic of Germany
(Received 25 October 1991)

Based on a suitable density-functional theory for inhomogeneous fluids we investigate both the liquid-vapor coexistence curve of the bulk phase diagram and interfacial structures of molecular fluids in general and Stockmayer fluids in particular. We derive a scheme which allows us to analyze one-component fluids composed of molecules with strong permanent dipole moments which are shown to affect significantly the bulk phase diagram. The critical temperature increases as a function of the strength of the dipole moments, whereas the critical density remains unchanged if the repulsive interaction of the molecules at short distances is modeled by a constant hard-core potential. A temperature-dependent diameter of the hard-core potential that mimics the actual soft repulsive potential is also considered. It results in an additional enhancement of the critical temperature and a slight increase of the critical density at larger dipole strengths and higher temperatures. Our analytic results turn out to be in good agreement with published Monte Carlo data. The density profile and the orientational ordering at interfaces are shown to be determined by a system of coupled integral equations that are applicable for dipole moments of arbitrary strength. Its corresponding numerical solution will be presented in a subsequent paper.

PACS number(s): 61.25.Em, 64.70.Fx, 68.10.Cr, 82.65.Dp

I. INTRODUCTION AND MOTIVATION

The understanding of the fluid state of matter poses a particular long-standing challenge of physics. Its peculiarity compared with other phases of condensed matter becomes evident by noting that in practical terms the difference between liquid and vapor is only visible when they are brought in contact with each other along their coexistence line in the bulk phase diagram, forming a liquid-vapor interface under the influence of gravity. The difficulties in describing a fluid can be attributed mainly to the absence of a lattice structure and to the fact that the interaction potential between individual atoms is on one side repulsive at short distances, and on the other side attractive at large distances, where it decays like a power law [1].

For about a century one has tried to understand fluids on the basis of statistical mechanics [2]. The large variety of methods that have been used signals that, in spite of remarkable successes, there is still no comprehensive exact solution available even for simple fluids whose atoms interact via spherically symmetric pair potentials [1]. The common wisdom is that one uses approximate methods that are tailored to address successfully a particular question one is interested in like, e.g., renormalization-group techniques in order to reveal universal phenomena close to the critical point T_c, sophisticated mean-field theories in order to investigate nonuniversal microscopic details, computer simulations for systems of finite size, etc. With these techniques a substantial amount of knowledge has been accumulated, in particular concerning the bulk phase diagram and the structure of the liquid-vapor interface [3]. Among the goals that have not yet been achieved even for simple fluids are (i) to have predictive theoretical power simultaneously for universal critical phenomena and nonuniversal microscopic details, and (ii) to reconcile in a satisfactory way the notion of an intrinsic interface profile corresponding to a flat interface with the occurrence of capillary waves at all length scales [4].

Another peculiarity of fluids is that they must be confined by solid walls. Both for theory and applications the structure of such solid-fluid interfaces is very interesting and important. This has led to a deeper understanding of fluids, because such interfaces require a description of fluids exposed to spatially varying external fields.

The discovery that such interfaces have the possibility to undergo structural phase transitions of their own has heightened the interest in that subject even further. In a wetting transition the solid-vapor interface splits into a solid-liquid and into a liquid-vapor interface accompanied by thermodynamic singularities of the wall-vapor surface tension [5–11].

It has turned out that among the variety of theoretical techniques that are used to describe strongly inhomogeneous fluids, only a few are capable of exhibiting the growth of a macroscopic wetting film. In that respect certain versions of the density-functional theory of fluids [12] are very successful: first- and second-order wetting transitions, complete wetting, prewetting, and the relation between the thermodynamic singularities of these transitions and the form of the interatomic interaction potentials have been established [5]–[11]. So far most of these theoretical investigations have been devoted only to simple fluids characterized by spherically symmetric pair

potentials. (Wetting studies of molecular fluids will be discussed separately and in more detail in the following sections.)

Rare gases represent the closest experimental realizations of such models. Indeed, numerous wetting experiments have been performed by adsorbing rare gases on solid substrates [6,7]. However, all of them are focused on temperatures below the triple point and deal with the wetting of the substrate by the solid phase of the adsorbate along its sublimation curve. There are also many experiments that investigate wetting phenomena above the triple point, even interfacial wetting in binary liquid mixtures [5–8,10]. However, all these latter experiments are performed with fluids composed of molecules that are far more complex than rare gases. In particular, these molecules have permanent electric multipole moments resulting in more complicated interaction potentials. The aforementioned theoretical wetting studies of simple fluids revealed already a surprisingly delicate dependence of wetting transitions on the strength, range, and form of the pair potentials [13]. Therefore one can expect that the additional presence of, e.g., orientational degrees of freedom and dipolar interactions is important for wetting transitions. Therefore an adequate theoretical understanding of the aforementioned wetting experiments with fluids requires us to take into account the molecular structure of the fluid particles. Since it turned out that the range of the interaction potentials is crucial for the nature of wetting phenomena [7], we pay particular attention to so-called Stockmayer fluids, whose special particles interact via dipolar and long-range van der Waals interactions. Nonetheless, our approach will allow us to also discuss certain aspects of molecular fluids in general, including liquid crystals.

Any analysis of wetting transitions requires one to solve simultaneously four problems: (i) the knowledge of the bulk phases, in particular the bulk phase diagram, (ii) the structure of the liquid-vapor interface, (iii) the structure of the solid-liquid interface, and finally (iv) the structure of the solid-vapor interface, which at a wetting transition transforms into a solid-liquid and into a liquid-vapor interface separated by a macroscopically thick liquid film.

The present paper addresses steps (i)–(iii) for molecular fluids and in particular for Stockmayer fluids. In the spirit of the second paragraph of this Introduction, our choice of the theoretical techniques is dictated by our goal to carry out the full program (i)–(iv) with one and the same method. In order to be able to accomplish this demanding task we are forced to introduce approximations that in parts go beyond those that would be necessary if one would only strive for solving each step (i)–(iii) separately without being interested in step (iv). Having this constraint in mind, we present results for bulk and interfacial structures of molecular and Stockmayer fluids.

In the following section we describe the model and the method we use in comparison with previous theoretical efforts in the literature. Section III deals with bulk properties of Stockmayer fluids, whereas Sec. IV is devoted to interfaces of such systems. In Sec. V we discuss the application of our approach to nematic liquids. Our results are summarized in Sec. VI. Appendix A contains a detailed comparison of both our approach and bulk results with the recent work by Teixeira and Telo da Gama [14]. Technical aspects, whose presentation is indispensable for understanding our approach, can be found in Appendix B. In Appendix C we discuss some details for applying the density-functional theory to nematic liquids.

II. MOLECULAR FLUIDS

In general, the molecules forming a liquid have nonspherical shapes and anisotropic pair potentials. Therefore, in contrast to simple fluids, there are not only positional but also orientational degrees of freedom. Their interplay leads to particularly rich interfacial phenomena.

The importance of the geometrical form of the molecules becomes apparent already in the bulk phases. If the aspect ratio of the molecules exceeds a critical value of about 2.45 [15], the fluid may exhibit orientational order without positional order, leading to the nematic phase of liquid crystals. Due to the technical importance of these materials, the preferential alignment of such molecules at interfaces has attracted considerable experimental and theoretical attention [16]. First efforts have been made at understanding wetting phenomena in liquid crystals on the basis of Landau theory [17] and density-functional theory [18,19]. Many studies are focused on the prominent steric interaction between the rodlike molecules whose pair potentials are taken to be invariant with respect to a rotation of 180° of one of them. Strictly speaking, in most cases this point symmetry is, however, violated, because the head and the tail of the molecule are different giving rise, among other things, to the presence of a permanent dipole moment. In many examples this property of liquid crystals seems to be of lesser importance because the dipole forces are relatively weak in comparison with the strong steric interactions. However, for smaller molecules these dipolar forces gain relative importance. In that spirit, we pay particular attention to polar fluids, confining our analysis to such molecules whose shapes can be approximated by spheres at the high temperatures and low densities in which we are interested. Nonetheless, our approach will be sufficiently general to allow us to comment also on molecular fluids that are characterized by *attractive* interaction potentials of arbitrary nonspherical form.

The bulk properties of dipolar fluids have been investigated by various methods. The principle of these investigations can be traced back to the seminal work of Keesom, who derived an averaged effective pair potential for dipolar molecules, which is temperature dependent and isotropic [20]. It is based on the assumption that the period of time in a molecular encounter is sufficiently long that the molecules can accomplish this averaging by their rotational motion. In that model a molecule experiences the potential of the other one averaged over all orientations rather than that given by the actual configuration. Among other things, such effective potentials have been used to study the critical behavior of polar fluids and have been refined in the framework of density-

functional theories in order to determine the equation of state [21–23] and the liquid-vapor coexistence curve [24]. In spite of the particular long range of the dipolar forces, the critical behavior of the bulk does not differ from that of nonpolar fluids with Lennard-Jones interactions, because at large distances the effective isotropic pair potential decays with the same r^{-6} power law [25]. Another approach, which is employed frequently, consists of the hypernetted-chain closure of the Ornstein-Zernicke or the Percus-Yevick equation and various refinements thereof. This framework allows one to calculate pair distribution functions, polarizabilities, dielectric constants, etc. [26–29]. In particular, Perera and Patey have studied the influence of point dipoles embedded in hard ellipsoids on their isotropic-nematic phase transition [30]. They employed a combination of hypernetted-chain and density-functional theories [31] and found the dipolar forces to have a significant effect on fluids consisting of prolate particles: The transition occurs at lower densities as the dipole moment is increased. For oblate molecules no definite effect could be established.

A. Interfaces of molecular fluids

The aforementioned hypernetted-chain integral-equation methods have also been used to investigate the structure of polar fluids in the vicinity of a neutral or charged wall [32,33]. Such interfaces induce not only nontrivial density profiles but also orientational order of the molecules, which causes the polarization to deviate from its bulk value.

A peculiarity of a system of dipoles near a dielectric wall is the emergence of image potentials that significantly affect the intermolecular dipole-dipole interaction even far from the wall. In a series of papers, Badiali and co-workers have addressed this problem [34]. Using an optimized cluster expansion, they derived analytical expressions for the potential of the mean force acting on a dipole both near and far from the wall.

Density-functional theories (DFT's) have also been employed to calculate density and polarization profiles of dipolar fluids in the vicinity of a charged wall or confined between two plates. The aim of these DFT studies by Woodward and Nordholm [35] and Moradi and Rickayzen [36] was to provide an understanding of the structure of polar solvents near immersed electrodes on a molecular level, thus improving the classical theory of the double layer [37].

While all of the aforementioned studies of the wall-liquid interface of polar fluids have been performed only recently, orientational profiles and surface tensions of free liquid-vapor interfaces of molecular fluids have been investigated for a long time [38]. Since we are particularly interested in the latter, we discuss these efforts in more detail than those devoted to the wall-liquid interface.

First theoretical approaches by Haile, Gray, and Gubbins were based on perturbation methods—the so-called u expansion—in which the surface tension [39] or the one-particle density [40] is expanded into powers of the anisotropic part of the intermolecular potential. At higher temperatures the former one becomes unreliable due to the Fowler approximation, which imposes a discontinuous number density profile at the surface. The latter approach was refined by Thompson and Gubbins [41], who were able to predict orientational ordering at a smooth interface due to overlap and dispersion forces in reasonably good agreement with molecular dynamic simulations. Both forces arise from a quantum-mechanical or semiclassical calculation of the ground state of a pair of molecules. The attractive dispersion forces are induced by a shift of the total electron charge density towards the intermolecular region, whereas the repulsive overlap forces are mainly due to the electronic exchange interaction [42], which, for anisotropic electron density distributions, gives rise to the short-range steric repulsion. In general, the anisotropy of these forces depends on the kind of molecules and differs from the symmetry of multipolarlike forces. However, the first term of the "u expansion" is *not* able to predict preferential ordering *for purely multipolarlike forces,* i.e., forces only due to anisotropic contributions of the multipole expansion of the electrostatic potential.

As an improvement, Thompson, Gubbins, and Haile [43] employed a perturbation theory in terms of the so-called f expansion, in which one expands in terms of the Mayer function of the anisotropic part of the potential. The first-order term is able to account for preferential ordering in the presence of purely multipolar forces due to the density change at the interface. However, within this approach both the number density profile and the surface tension are determined by the isotropic part of the potential only and are thus unaffected by the orientational order at the interface.

Tarazona and Navascués [44] developed an alternative approach, which employs a perturbative expansion for the Helmholtz free energy in powers of the anisotropic part of the potential to first order. This allows them to simultaneously determine the effect of the anisotropic forces to the mean molecular orientation and to the surface tension. However, since one is expanding in terms of the anisotropic part of the potential itself, this theory was likewise unable to account for ordering induced by purely multipolar intermolecular forces in the absence of external fields or anisotropic dispersion or anisotropic overlap interactions. As before, the density profile is not coupled to the orientation profile, preventing a feedback of the orientational order at the surface to the thickness of the interface. A subsequent generalization of the theory in terms of a density-functional formalism [45] also suffers from these drawbacks.

The recent work of Eggebrecht, Gubbins, and Thompson [46] is devoted to Stockmayer fluids, i.e., the anisotropic part of the potential is taken to be purely dipolelike. They used Yvon-Born-Green integral equations and f-expansion perturbation theories, which both yield a preferential orientational order at the interface: The molecules tend to lie parallel to the surface on the liquid side of the interface, which is in qualitative agreement with molecular-dynamics simulations carried out by the same authors [47]. On the gas side of the interface the molecules prefer to orientate perpendicular to the interface according to the analytic theory, whereas the simulation

does not yield a definitive orientation here. Thus the occurrence of a preferential orientation at an interface induced by purely multipolar forces is established. In addition, the increase of the surface tension with stronger dipole moments has been observed.

More recently, within the framework of a density-functional approach, Teixeira and Telo da Gama [14] achieved similar results. They employed a so-called modified mean-field approximation using the low-density limit of the pair distribution function entering the density functional instead of its large-distance limit as it is used in the simplest version of this mean-field theory. Within this approach, the exponential function of the ratio of the long-range part of the intermolecular interaction and $k_B T$ enters the free-energy functional. By expanding this exponential function to second order and simultaneously minimizing the grand-canonical functional with respect to the number density *and* the orientation profile, they obtained for the first time a nontrivial coupling of the density profile to the molecular orientation at the interface. Generally speaking, they corroborated the results of Eggebrecht, Gubbins, and Thompson and obtained a preference for parallel orientation on the liquid side and a preference for perpendicular orientation on the gas side of the interface. However, for the small dipole strengths they used, the deviation from isotropy turns out to be only a few percent.

A major shortcoming of all the theories mentioned above is that they are restricted to small dipole or multipole strengths. This is due to the aforementioned truncation of the expansion in terms of the anisotropic potential (or its corresponding Mayer function) in the perturbation theories or of the series expansion of the exponential of the long-range part of the potential in the density-functional formalism, respectively. Such truncations do not only affect the interfacial properties, such as the orientational order and the surface tension, but they influence considerably even the bulk phase diagram. Since, as emphasized in the Introduction, the liquid-vapor coexistence in the bulk is the starting point for investigations concerning the wetting behavior of fluids, it is desirable to provide more reliable methods.

It is well known that DFT's are suitable tools to describe wetting transitions, whereas the aforementioned integral-equation methods fail to predict the emergence of a macroscopically thick wetting film of a third phase growing at the interface between two coexisting thermodynamic phases [48]. Since the DFT is appropriate for carrying out all the other steps (i)–(iv) mentioned in the Introduction, we seek to improve and apply this approach for molecular fluids. A detailed comparison of bulk quantities as obtained by our approach versus the one used by Teixeira and Telo da Gama [14] is given in Appendix A.

1. *Density-functional theory for molecular fluids*

In a one-component inhomogeneous and anisotropic fluid, $\hat{\rho}(\mathbf{r},\omega)$ denotes the number density of particles at the point $\mathbf{r}=(x,y,z)$ that have an orientation $\omega=(\theta,\phi)$ with respect to the space fixed coordinate system (see Fig. 1). The total number density of particles without specified orientation is given by

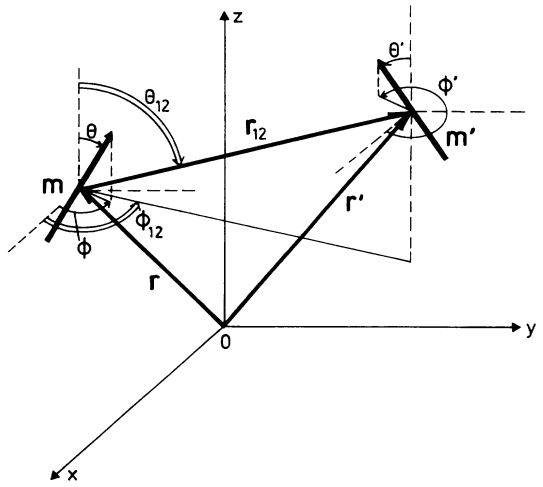

FIG. 1. Illustration of the geometry in a spatially fixed reference frame. $\omega=(\theta,\phi)$ and $\omega'=(\theta',\phi')$ denote the orientation of the dipole moments $\mathbf{m}$ and $\mathbf{m}'$, respectively. $\omega_{12}=(\theta_{12},\phi_{12})$ is the orientation of the intermolecular vector $\mathbf{r}_{12}$. The interface is parallel to the xy plane.

$$\rho(\mathbf{r})=\int d\omega\,\hat{\rho}(\mathbf{r},\omega)=\int_0^{2\pi}d\phi\int_0^{\pi}d\theta\,(\sin\theta)\hat{\rho}(\mathbf{r},\theta,\phi)\ . \quad (2.1)$$

This allows us to split $\hat{\rho}$ into the total number density ρ and a normalized space- and angle-dependent factor α:

$$\hat{\rho}(\mathbf{r},\omega)=\rho(\mathbf{r})\alpha(\mathbf{r},\omega),\quad \int d\omega\,\alpha(\mathbf{r},\omega)=1\ . \quad (2.2)$$

In the presence of an external potential $V_{\text{ext}}(\mathbf{r},\omega)$, the grand-canonical free energy for such a given configuration is

$$\begin{aligned}\Omega[\{\hat{\rho}(\mathbf{r},\omega)\},T,\mu]=&\mathcal{F}[\{\hat{\rho}(\mathbf{r},\omega)\},T]\\&+\int d^3r\,d\omega\,\hat{\rho}(\mathbf{r},\omega)V_{\text{ext}}(\mathbf{r},\omega)\\&-\mu\int d^3r\,d\omega\,\hat{\rho}(\mathbf{r},\omega)\ , \end{aligned}\quad (2.3)$$

where $\mathcal{F}[\{\hat{\rho}(\mathbf{r},\omega)\},T]$ represents the Helmholtz free-energy functional for this configuration; μ is the chemical potential. The actual grand-canonical free energy is the minimum of the variational functional and determines the equilibrium density configuration:

$$\begin{aligned}\Omega(T,\mu)=&\min_{\hat{\rho}(\mathbf{r},\omega)}\Omega[\{\hat{\rho}(\mathbf{r},\omega)\},T,\mu]\\=&\Omega[\{\hat{\rho}_{\text{eq}}(\mathbf{r},\omega;T,\mu)\},T,\mu]\ , \end{aligned}\quad (2.4)$$

obtained by

$$\left.\frac{\delta\Omega[\{\hat{\rho}(\mathbf{r},\omega)\},T,\mu]}{\delta\hat{\rho}(\mathbf{r},\omega)}\right|_{\hat{\rho}(\mathbf{r},\omega)=\hat{\rho}_{\text{eq}}(\mathbf{r},\omega;T,\mu)}=0\ . \quad (2.5)$$

By using Eq. (2.2) it can be shown that Eq. (2.5) is equivalent to the simultaneous minimization of the grand-canonical functional with respect to the total number density ρ,

$$\left.\frac{\delta\Omega[\{\hat{\rho}(\mathbf{r},\omega)\},T,\mu]}{\delta\rho(\mathbf{r})}\right|_{\rho(\mathbf{r})=\rho_{\mathrm{eq}}(\mathbf{r};T,\mu)}=0\ , \tag{2.6}$$

and the orientational configuration $\alpha(\mathbf{r},\omega)$,

$$\left.\frac{\delta\Omega[\{\hat{\rho}(\mathbf{r},\omega)\},T,\mu]}{\delta\alpha(\mathbf{r},\omega)}\right|_{\alpha(\mathbf{r},\omega)=\alpha_{\mathrm{eq}}(\mathbf{r},\omega;T,\mu)}=0\ . \tag{2.7}$$

The Helmholtz-free-energy functional $\mathcal{F}$ can be written as a sum of the free energy $\mathcal{F}_{\mathrm{ref}}$ of a reference system characterized by a purely isotropic interaction potential $w_{\mathrm{ref}}(\mathbf{r},\mathbf{r}')$ and an excess free energy

$$\mathcal{F}_{\mathrm{ex}}[\{\hat{\rho}(\mathbf{r},\omega)\},T]=\mathcal{F}[\{\hat{\rho}(\mathbf{r},\omega)\},T]-\mathcal{F}_{\mathrm{ref}}[\{\hat{\rho}(\mathbf{r},\omega)\},T] \tag{2.8}$$

due to that part of the intermolecular interaction which is not present in the reference system. This allows one to choose a convenient reference system for which exact expressions or at least reliable approximations for the free energy are known.

By using functional integration, the excess free energy can be expressed in terms of the two-particle density:

$$\hat{\rho}^{(2)}(\mathbf{r},\mathbf{r}',\omega,\omega',\alpha,T)=\left\langle \sum_{\substack{i,j\\ i\neq j}}\delta(\mathbf{r}-\mathbf{r}_i)\delta(\omega-\omega_i)\delta(\mathbf{r}'-\mathbf{r}_j)\delta(\omega'-\omega_j)\right\rangle$$
$$=\langle\hat{\rho}(\mathbf{r},\omega)\rangle\langle\hat{\rho}(\mathbf{r},\omega')\rangle g^{(2)}(\mathbf{r},\mathbf{r}',\omega,\omega')\ . \tag{2.9}$$

The angular brackets $\langle\ \rangle$ denote the thermal average. For pairwise intermolecular potentials $w(\mathbf{r},\mathbf{r}',\omega,\omega')$ one has

$$\hat{\rho}^{(2)}(\mathbf{r},\mathbf{r}',\omega,\omega',\alpha,T)=2\frac{\delta\mathcal{F}[\{\hat{\rho}_{\mathrm{eq}}(\mathbf{r},\omega),T]}{\delta w(\mathbf{r},\mathbf{r}',\omega,\omega')}\ , \tag{2.10}$$

so that the Helmholtz free energy is given by [12]

$$\mathcal{F}[\{\hat{\rho}_{\mathrm{eq}}(\mathbf{r},\omega)\},T]=\mathcal{F}_{\mathrm{ref}}[\{\hat{\rho}_{\mathrm{eq}}(\mathbf{r},\omega)\},T]$$
$$+\tfrac{1}{2}\int_0^1 d\alpha\int\int d^3r\,d^3r'\,d\omega\,d\omega' g^{(2)}(\mathbf{r},\mathbf{r}',\omega,\omega',\alpha,T)\hat{\rho}_{\mathrm{eq}}(\mathbf{r},\omega)\hat{\rho}_{\mathrm{eq}}(\mathbf{r}',\omega')w_{\mathrm{ex}}(\mathbf{r},\mathbf{r}',\omega,\omega')\ , \tag{2.11}$$

with the excess contribution to the intermolecular potential

$$w_{\mathrm{ex}}(\mathbf{r},\mathbf{r}',\omega,\omega')=w(\mathbf{r},\mathbf{r}',\omega,\omega')-w_{\mathrm{ref}}(\mathbf{r},\mathbf{r}') \tag{2.12}$$

and a pair distribution function $g^{(2)}(\mathbf{r},\mathbf{r}',\omega,\omega',\alpha,T)$ of an inhomogeneous fluid with a pairwise intermolecular potential parametrized by α:

$$w_\alpha(\mathbf{r},\mathbf{r}',\omega,\omega')=w_{\mathrm{ref}}(\mathbf{r},\mathbf{r}')+\alpha[w(\mathbf{r},\mathbf{r}',\omega,\omega')-w_{\mathrm{ref}}(\mathbf{r},\mathbf{r}')]\ . \tag{2.13}$$

2. *Approximations*

Equation (2.11) is an exact expression for the excess free energy. However, in general the pair distribution function $g^{(2)}$ is not known for inhomogeneous fluids. All approximations known so far lead to mean-field-like theories, i.e., they do not capture the nonclassical behavior close to T_c or the roughening of fluid interfaces due to capillary waves in the absence of gravity (see the second paragraph of the Introduction). However, as far as continuous wetting transitions are concerned, the capillary waves are irrelevant for the corresponding thermal singularities if the system is governed by long-range forces [49].

Among these known approximations for $g^{(2)}$ there exist elaborate ones for homogeneous systems and interpolations between those of different homogeneous states of the fluid, but they create considerable computational difficulties in the case of inhomogeneous systems. The simplest approximation, which still captures the essential features of wetting phenomena [13], consists of taking the large-distance limit $g^{(2)}=1$. However, in the present context this ignorance of local correlations is too crude an approximation. Due to the symmetry of purely multipolar pair potentials, the excess free energy of a homogeneous bulk phase vanishes for $g^{(2)}=1$:

$$\mathcal{F}_{\mathrm{ex},b}^{\mathrm{mult}}=\tfrac{1}{2}\rho^2\int\int d^3r\,d^3r'\,d\omega\,d\omega' w_{\mathrm{ex}}^{\mathrm{mult}}(\mathbf{r},\mathbf{r}',\omega,\omega')=0\ . \tag{2.14}$$

Hence the bulk phase diagram is unaffected by any multipole moments, independent of their strengths. This apparently unrealistic feature leads us to take into account at least two-point correlation functions in the excess free energy while retaining a simple structure in order to facilitate subsequent studies of wetting phenomena.

As a trade of balance, we take the bulk pair distribution function in its low-density limit,

$$g^{(2)}(\mathbf{r},\mathbf{r}',\omega,\omega',\alpha,T)=e^{-\beta w_\alpha(\mathbf{r},\mathbf{r}',\omega,\omega')}\ ,$$
$$\beta=\frac{1}{k_BT}\ , \tag{2.15}$$

which leads to an excess free energy in the so-called modified mean-field approximation [14]:

$$\mathcal{F}_{ex}[\{\hat{\rho}(\mathbf{r},\omega)\},T] = \frac{1}{2\beta}\int\int d^3r\, d^3r' d\omega d\omega' \hat{\rho}(\mathbf{r},\omega)\hat{\rho}(\mathbf{r}',\omega') \times e^{-\beta w_{ref}(\mathbf{r},\mathbf{r}')}(1-e^{-\beta w_{ex}(\mathbf{r},\mathbf{r}',\omega,\omega')}) . \tag{2.16}$$

As will be shown in the next subsection, the reference free energy $\mathcal{F}_{ref}[\{\hat{\rho}(\mathbf{r},\omega)\},T]$ [see Eq. (2.8)] is the sum of $\mathcal{F}_{ref}^{HS}[\{\hat{\rho}(\mathbf{r},\omega)\},T]$ and $\mathcal{F}_{ref}^{or}[\{\hat{\rho}(\mathbf{r},\omega)\},T]$. The hard-sphere reference free energy $\mathcal{F}_{ref}^{HS}$ is due to both the contribution of the short-range repulsive forces to the internal energy and to the configurational entropy of the reference system in the absence of orientational degrees of freedom. $\mathcal{F}_{ref}^{or}$ takes into account that there are orientational degrees of freedom in the reference system, which, however, by construction do not interact with each other, because w_{ref} does not depend on ω or ω'. In the following we treat $\mathcal{F}_{ref}^{HS}$ in the local-density approximation

$$\mathcal{F}_{ref}^{HS}[\{\rho(\mathbf{r})\},T] = \int d^3r\, f_{ref}^{HS}(\rho(\mathbf{r}),T) , \tag{2.17}$$

where $f_{ref}^{HS}(\rho,T)$ is the Helmholtz free-energy density of a homogeneous bulk phase with density ρ. This approximation is reliable for smooth density variations as they occur at the liquid-vapor interface. (The local structure of a fluid near a wall is captured only crudely by this approximation, whereas the long-range van der Waals tails, which are important for wetting phenomena, are given correctly [13].) By taking into account the normalization condition for the orientational distribution [see Eq. (2.2)] by a Lagrange parameter $\kappa(\mathbf{r})$, one finally obtains the following expression for the grand-canonical variational potential:

$$\begin{aligned}\Omega[\{\hat{\rho}(\mathbf{r},\omega)\},T,\mu] = &\int d^3r\, f_{ref}^{HS}(\rho(\mathbf{r}),T) + \mathcal{F}_{ref}^{or}[\{\hat{\rho}(\mathbf{r},\omega)\},T] \\ &+ \frac{1}{2\beta}\int\int d^3r\, d^3r' d\omega\, d\omega' \rho(\mathbf{r})\rho(\mathbf{r}')\alpha(\mathbf{r},\omega)\alpha(\mathbf{r}',\omega') e^{-\beta w_{ref}(\mathbf{r},\mathbf{r}')}(1-e^{-\beta w_{ex}(\mathbf{r},\mathbf{r}',\omega,\omega')}) \\ &+ \int d^3r\, d\omega V_{ext}(\mathbf{r},\omega)\rho(\mathbf{r})\alpha(\mathbf{r},\omega) - \mu\int d^3r\, d\omega\, \rho(\mathbf{r})\alpha(\mathbf{r},\omega) + \int d^3r\, \kappa(\mathbf{r})\left[1-\int d\omega\, \alpha(\mathbf{r},\omega)\right] . \end{aligned} \tag{2.18}$$

The equilibrium value of the Lagrange parameter $\kappa(\mathbf{r},T,\mu)$ follows from the normalization condition for the orientational distribution.

B. The Stockmayer fluid as a model system

Within the limits set by the aforementioned approximations, Eq. (2.18) is valid for molecular fluids in general. In this subsection we want to study it for the so-called Stockmayer model of a one-component polar fluid, which consists of spherically shaped molecules interacting via a Lennard-Jones potential to which an interaction is added due to point dipoles embedded in the spheres. This dipole-dipole interaction is assumed to act only outside of a hard-sphere diameter d, which depends on a suitable decomposition of the Lennard-Jones potential into a purely repulsive short-range interaction w_{ref} and a long-range attractive interaction $\hat{w}$. For computational convenience we choose the decomposition due to Barker and Henderson [50], where the hard-sphere diameter d coincides with the Lennard-Jones parameter σ:

$$w_{ref}(r_{12}) = \begin{cases} w_{LJ}(r_{12}), & r_{12} \le \sigma \\ 0, & r_{12} > \sigma , \end{cases}$$

$$\hat{w}(r_{12}) = \begin{cases} 0, & r_{12} \le \sigma \\ w_{LJ}(r_{12}), & r_{12} > \sigma , \end{cases} \tag{2.19}$$

where w_{LJ} denotes the Lennard-Jones potential

$$w_{LJ}(r_{12}) = 4\epsilon\left[\left(\frac{\sigma}{r_{12}}\right)^{12} - \left(\frac{\sigma}{r_{12}}\right)^{6}\right] . \tag{2.20}$$

In the absence of the dipolar interaction, $\hat{w}$ would be equal to w_{ex}, introduced in the previous subsection. The dipole-dipole interaction

$$w_{dip}(\mathbf{r},\mathbf{r}',\omega,\omega') = w_{dip}(\mathbf{r}_{12}=\mathbf{r}-\mathbf{r}',\omega,\omega') = \begin{cases} 0, & r_{12} \le \sigma \\ -\mathbf{m}(\omega)\mathbf{T}(\mathbf{r}_{12})\mathbf{m}(\omega'), & r_{12} > \sigma \end{cases} \tag{2.21}$$

is given by the dipole moment $\mathbf{m}(\omega)$ of the molecules in a spatially fixed reference frame and by the interaction tensor $\mathbf{T}(\mathbf{r}_{12})$ with the tensor elements

$$\mathbf{T}_{\alpha\beta}(\mathbf{r}_{12}) = \frac{3(\mathbf{r}_{12})_\alpha(\mathbf{r}_{12})_\beta}{r_{12}^5} - \frac{\delta_{\alpha\beta}}{r_{12}^3} . \tag{2.22}$$

Upon construction, w_{dip} adds only to $\hat{w}$, so that w_{ex} is given by

$$w_{ex}(\mathbf{r},\mathbf{r},\omega,\omega')=\begin{cases}0, & r_{12}\leq\sigma\\ 4\epsilon\left[\left(\frac{\sigma}{r_{12}}\right)^{12}-\left(\frac{\sigma}{r_{12}}\right)^{6}\right]-\frac{m^2}{r_{12}^3}\left[\frac{3[\hat{\mathbf{m}}(\omega)\mathbf{r}_{12}][\hat{\mathbf{m}}(\omega')\mathbf{r}_{12}]}{r_{12}^2}-\hat{\mathbf{m}}(\omega)\hat{\mathbf{m}}(\omega')\right], & r_{12}>\sigma\ ,\end{cases} \tag{2.23}$$

m is the absolute value of the dipole moment, and $\hat{\mathbf{m}}(\omega)$ is its unit vector.

Up to this point the reference system is governed by the repulsive part of the Lennard-Jones potential. In order to proceed, this reference system is now replaced by a system of hard spheres [51] of diameter $d=\sigma$. For this system an approximate expression for the Helmholtz free-energy density has been given by Carnahan and Starling [52]:

$$f_{\text{ref}}^{\text{HS,CS}}(\rho,T)=\frac{1}{\beta}\rho\left[\ln(\rho\lambda^3)-1+\frac{4\eta-3\eta^2}{(1-\eta)^2}\right]\ ; \tag{2.24}$$

λ is the thermal de Broglie wavelength and $\eta=(\pi/6)d^3\rho$ denotes the packing fraction.

Equation (2.24) holds for structureless hard spheres. However, in the present case, each sphere is tagged by its embedded dipole moment, which can point in any direction ω. Thus every total density configuration $\rho(\mathbf{r})$ encompasses all possible orientations of the spheres. This enhancement of the phase space leads to an extra contribution to the entropy of the reference system [19]

$$\mathcal{F}_{\text{ref}}^{\text{or}}[\{\hat{\rho}(\mathbf{r},\omega)\},T]=\frac{1}{\beta}\int d^3r\,\rho(\mathbf{r})\int d\omega\,\alpha(\mathbf{r},\omega)\ln[4\pi\alpha(\mathbf{r},\omega)]\ , \tag{2.25}$$

which vanishes in the case of an isotropic distribution $\alpha(\mathbf{r},\omega)=1/4\pi$. Thus the Helmholtz free energy of the reference system is given by

$$\mathcal{F}_{\text{ref}}[\{\hat{\rho}(\mathbf{r},\omega)\},T]=\frac{1}{\beta}\int d^3r\,\rho(\mathbf{r})\left[\ln\rho(\mathbf{r})\lambda^3-1+\frac{4\eta-3\eta^2}{(1-\eta)^2}+\int d\omega\,\alpha(\mathbf{r},\omega)\ln[4\pi\alpha(\mathbf{r},\omega)]\right]. \tag{2.26}$$

Finally, we refine our reference system by introducing a temperature-dependent hard-sphere diameter $d(T)$, employing the Barker-Henderson formula [53]

$$d(T)=\int_0^\infty dr(1-e^{-\beta w_{\text{ref}}(r)})\ . \tag{2.27}$$

This mimics the actually soft repulsive part of the Lennard-Jones intermolecular potential.

III. BULK PROPERTIES OF STOCKMAYER FLUIDS

Depending on temperature, pressure, and the strength m of the dipole moment, the Stockmayer model allows for a variety of stable bulk phases that exhibit either spatial and orientational order (ferroelectric or antiferroelectric phases), spatial order without orientational order (paraelectric phases), or spatial and orientational disorder (fluid phases). Whereas the former phases require the formation of a solid with various lattice structures, one can speculate whether the Stockmayer model allows for a spontaneous orientational order without a long-range spatial order. (The possibility of the emergence of a ferroelectric nematic phase for hard ellipsoids with point dipoles embedded is discussed in Refs. [30] and [54].) In this paper we consider only those values of the external parameters for which, in the absence of external fields, i.e., $V_{\text{ext}}(\mathbf{r},\omega)=0$, a homogeneous and isotropic bulk phase is formed:

$$\rho(\mathbf{r})=\text{const}\quad\text{and}\quad\alpha(\mathbf{r},\omega)=\frac{1}{4\pi}\ . \tag{3.1}$$

Under these circumstances there are no depolarization effects. From Eqs. (2.18) and (2.26) we obtain the bulk expression for the grand-canonical potential:

$$\frac{\Omega_b(\rho,T,\mu)}{V}=f_{\text{HS}}^{\text{CS}}(\rho)+\tfrac{1}{2}\rho^2U(T)-\mu\rho\ . \tag{3.2}$$

The bulk densities $\rho_b(T,\mu)$ follow from $[\partial\Omega_b(\rho,T,\mu)/\partial\rho]|_{\rho=\rho_b(T,\mu)}=0$, so that the pressure $p(T,\mu)$ is determined by $p=-\Omega_b(\rho_b(T,\mu),T,\mu)/V$. U contributes to the internal energy, and within the present model it is given by

$$U(T)=\frac{4\pi}{\beta}\int_0^\infty dr_{12}r_{12}^2e^{-\beta w_{\text{ref}}(r_{12})}\times(1-\langle e^{-\beta w_{\text{ex}}(\mathbf{r}_{12},\omega,\omega')}\rangle_{\omega\omega'})\ , \tag{3.3}$$

with w_{ex} defined in Eq. (2.23) and where $\langle A\rangle_{\omega\omega'}$ denotes the average of a quantity $A(\omega,\omega')$ over the unit sphere S_2:

$$\langle A\rangle_{\omega\omega'}=\frac{1}{(4\pi)^2}\int_{S_2}d\omega\int_{S_2}d\omega'\,A(\omega,\omega')\ . \tag{3.4}$$

For w_{ex} in Eq. (2.23) one can show that $\langle e^{-\beta w_{\text{ex}}(\mathbf{r}_{12},\omega,\omega')}\rangle_{\omega\omega'}$ is indeed a function of $r_{12}=|\mathbf{r}_{12}|$. Due to the Barker-Henderson decomposition of the intermolecular potential, the expression in Eq. (3.3) reduces to

$$U(T)=\frac{1}{\beta}4\pi\int_\sigma^\infty dr_{12}r_{12}^2\left[1-e^{-\beta w_{\text{LJ}}(r_{12})}\times\langle e^{-\beta w_{\text{dip}}(\mathbf{r}_{12},\omega,\omega')}\rangle_{\omega\omega'}\right]. \tag{3.5}$$

A. Effective isotropic dipole-dipole interaction potential

Equation (3.5) allows one to define an effective dipole-dipole interaction potential

$$\bar{w}_{\rm dip}(r_{12}) = -k_B T \ln\langle e^{-\beta \mathbf{m}\cdot\mathbf{T}\cdot\mathbf{m}'}\rangle_{\omega\omega'} , \tag{3.6}$$

which, according to our above statement, is indeed isotropic. We evaluate it by means of a Taylor-series expansion of $e^{-\beta \mathbf{m}\cdot\mathbf{T}\cdot\mathbf{m}'}$ in terms of the dimensionless strength $Z=\beta m^2/r_{12}^3$ of the interaction of a pair of dipoles with moments m separated by a distance r_{12} at a temperature T. In contrast to other authors [14], we do not truncate the series after the second term, but we employ a method recently described by Mercer [55] that yields analytically exact expressions for the effective isotropic interaction. In addition, this method offers computational advantages by avoiding separate integration procedures for different values of r_{12}, m, and T. As shown in Appendix A for the model used by Teixeira and Telo da Gama [14], these higher-order terms in the expansion of $\bar{w}_{\rm dip}$ influence the bulk phase diagram significantly.

Since the angular average of odd powers of the dipole-dipole interaction vanishes, one has

$$\langle e^{-\beta \mathbf{m}\cdot\mathbf{T}\cdot\mathbf{m}'}\rangle_{\omega\omega'} = \sum_{n=0}^{\infty} \frac{(\langle \hat{\mathbf{m}}\cdot\hat{\mathbf{T}}\cdot\hat{\mathbf{m}}'\rangle_{\omega\omega'})^{2n}}{(2n)!} Z^{2n} , \tag{3.7}$$

where $\hat{\mathbf{T}}=\mathbf{T}r_{12}^3$ is dimensionless. By using the vector and tensor properties of the integrand entering the angular average, one can derive the following integral representation for the Taylor-series coefficients [55]:

$$\frac{(\langle \hat{\mathbf{m}}\cdot\hat{\mathbf{T}}\cdot\hat{\mathbf{m}}'\rangle_{\omega\omega'})^{2n}}{(2n)!} = \frac{1}{(2n+1)!}\int_0^1 dx\,(1+3x^2)^n . \tag{3.8}$$

Substituting this into Eq. (3.7), the series can be expressed in terms of a single integral

$$\langle e^{-\beta w_{\rm dip}(\mathbf{r}_{12},\omega,\omega')}\rangle_{\omega\omega'} = \int_0^1 dx\, i_0[Z(1+3x^2)^{1/2}] , \tag{3.9}$$

where $i_0(y)=\sinh y/y$ is the modified spherical Bessel function of zero order [56]. Note that $i_0(y)$ depends only on *even* powers of y. Appropriate recursion relations [55] lead to another representation:

$$\langle e^{-\beta w_{\rm dip}(\mathbf{r}_{12},\omega,\omega')}\rangle_{\omega\omega'} = \sum_{n=0}^{\infty}\left[\frac{2^n n!}{(2n+1)!}\right]^2 \sum_{k=0}^{n}\binom{2k}{k} Z^{2n} , \tag{3.10}$$

which is convenient for numerical computation because its convergence can easily be controlled. For $Z\le 4$ the truncation at $n=15$ gives rise to a relative error of less than 10^{-6}.

From this representation one can easily derive the asymptotic behavior of the isotropic effective dipole-dipole potential for $r_{12}\to\infty$, i.e., $Z\to 0$ [57]:

$$\bar{w}_{\rm dip}(Z) = -k_B T\left(\tfrac{1}{3}Z^2 - \tfrac{7}{450}Z^4 + \tfrac{163}{99\,235}Z^6 - \cdots + \cdots\right) . \tag{3.11}$$

In terms of the intermolecular distance r_{12} one has

$$\bar{w}_{\rm dip}(r_{12};T,m) = -\frac{a}{r_{12}^6} + \frac{b}{r_{12}^{12}} - \frac{c}{r_{12}^{18}} + \cdots - \cdots , \tag{3.12}$$

with

$$a=\frac{\beta m^4}{3},\quad b=\frac{7\beta^3 m^8}{450},\quad c=\frac{163\beta^5 m^{12}}{99\,235} . \tag{3.13}$$

We stress that, according to the definition of $w_{\rm dip}$ given above [see Eq. (2.21)], $\bar{w}_{\rm dip}=0$ for $r_{12}<\sigma$. For $r_{12}\ge\sigma$ the effective pair potential $\bar{w}_{\rm dip}$ is attractive throughout its entire range. Figure 2 shows $\bar{w}_{\rm dip}/k_B T$ as a function of the dimensionless distance $\bar{r}=Z^{-1/3}=[k_b T/\epsilon/(m^*)^2]^{1/3} r_{12}/\sigma$, were $m^*=(m^2/\sigma^3\epsilon)^{1/2}$ is the dimensionless dipole strength. The lower bound $\bar{r}_{\rm min}=0.55$ of this distance is determined by (i) $r_{12}\ge\sigma$ due to the definition of the dipole-dipole potential, (ii) $m^*\le 2$, which is the range of dimensionless dipole moments we consider, and (iii) $k_B T/\epsilon>0.68$, since the triple temperature of the pure Lennard-Jones fluid (i.e., for $m=0$) is $T_3=0.68\epsilon/k_B$ [58]. The triple temperature imposes also a lower limit on the temperature range for the liquid-vapor coexistence curve. The relative strength $a/(4\epsilon\sigma^6)$ of the effective dipole-dipole potential with respect to the Lennard-Jones potential decreases from $0.123(m^*)^4$ at $T_3(m^*=0)$ to $0.067(m^*)^4$ at $T_c(m^*=0)$ (see Table I). Thus for $m^*>1$ the effect of the dipole interaction potential is increasingly important.

B. Liquid-vapor coexistence

The liquid (l)-gas (g) phase diagram follows from the requirement that at a given temperature T both the pressure and the chemical potential in the two phases are equal:

$$\Omega_b(\rho_g,T,\mu) = \Omega_b(\rho_l,T,\mu) \tag{3.14}$$

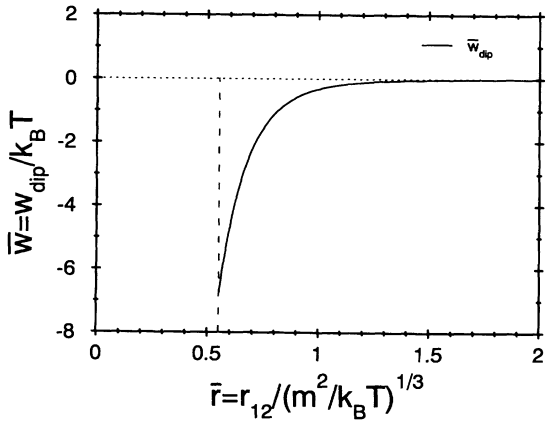

FIG. 2. The effective isotropic dipole-dipole potential as a function of the dimensionless distance $\bar{r}=Z^{-1/3}=r_{12}/(m^2/k_b T)^{1/3}$. The cutoff at $\bar{r}_{\rm min}=0.55$ is due to the natural constraints explained in the main text. At large distances the effective potential decays $\sim\bar{r}^{-6}$ as the Lennard-Jones potential does.

TABLE I. Bulk critical values for the density $\rho_c^* = \rho_c \sigma^3$, the temperature $T_c^* = k_B T_c / \epsilon$, and the chemical potential $\mu_c^* = \mu_c / \epsilon$ for various dipole strengths m^* of Stockmayer fluids with hard-sphere diameter $d = \sigma$.

m^*	ρ_c^*	T_c^*	μ_c^*
0.0	0.2491	1.2358	−4.2489
0.5	0.2491	1.2440	−4.2772
1.0	0.2491	1.3566	−4.6643
1.5	0.2491	1.7180	−5.9077
2.0	0.2491	2.3508	−8.0826

$$\left.\frac{\partial \Omega_b(\rho,T,\mu)}{\partial \rho}\right|_{\rho=\rho_g(T,\mu)} = \left.\frac{\partial \Omega_b(\rho,T,\mu)}{\partial \rho}\right|_{\rho=\rho_l(T,\mu)} = 0 \,. \tag{3.15}$$

In order to test the reliability of our approximations we compare for a pure Lennard-Jones fluid (i.e., $m=0$) the predictions of the DFT as described above with recent Monte Carlo simulations [59] (see Fig. 3). The agreement between the Monte Carlo data and the analytic theory with a temperature-dependent hard-sphere diameter is rather satisfying. As expected, at higher densities the DFT in its present form overestimates the liquid density due to the low-density approximation for the pair distribution function [see Eq. (2.15)].

Figure 4 displays the liquid-vapor coexistence curve of Stockmayer fluids with various dimensionless dipole strengths m^*, $0 \le m^* \le 2$. These results are obtained by using a hard-sphere reference system. The values for ρ, T, and μ at the critical point are given in Table I. They result from consecutively solving the following equations:

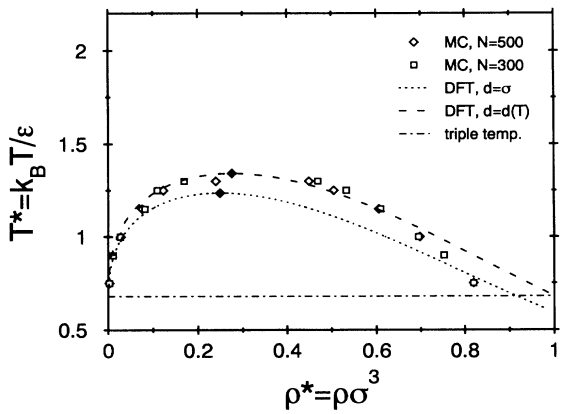

FIG. 3. Liquid-vapor phase diagram for a Lennard-Jones fluid as obtained by Monte Carlo simulations (MC) by Panagiotopoulos [59] with samples of 300 and 500 particles, respectively, compared with the predictions of the present density-functional theory (DFT) with temperature-independent ($d=\sigma$) and temperature-dependent [$d=d(T)$] hard-sphere diameter. The triple temperature is indicated [58]. The dot denotes the critical point $(T_c^*, \rho_c^*) = (1.3430, 0.2757)$ according to the DFT with $d=d(T)$.

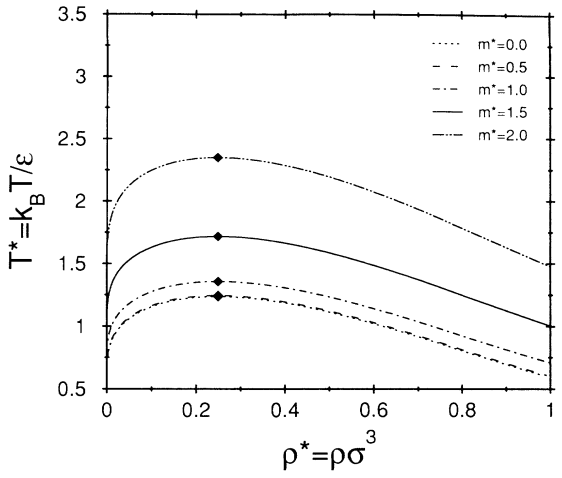

FIG. 4. Liquid-vapor phase diagrams of Stockmayer fluids with various dipole strengths m^* in the hard-sphere version of the DFT. The dots denote the critical points.

$$\left.\frac{\partial^3 \Omega_b}{\partial \rho^3}\right|_{\rho_c} = 0, \quad \left.\frac{\partial^2 \Omega_b}{\partial \rho^2}\right|_{\rho_c, T_c} = 0, \quad \left.\frac{\partial \Omega_b}{\partial \rho}\right|_{\rho_c, T_c, \mu_c} = 0 \,. \tag{3.16}$$

The critical temperature is raised by increasing the strength of the dipole moments. In the hard-sphere version the critical density does not depend on m^* because it is determined by the third derivative of the grand-canonical potential, which involves only the reference system carrying no m^* dependence.

As in the case of a pure Lennard-Jones fluid (see Fig. 3), a temperature-dependent hard-sphere diameter [see Eq. (2.27)] leads to an enhancement of the critical temperature. This is shown in Fig. 5 and can be read off by comparing Tables I and II.

In Table II the critical densities are larger than in Table I and they increase for larger dipole moments. This shift is caused by the increase of T_c as a function of m, which leads to a smaller temperature-dependent effective hard-sphere diameter at T_c [see Eq. (2.27)].

For the special case $m^* = 1.0$, Fig. 6 compares our results with recent Monte Carlo simulations by Smit *et al.* [60]. As in the case of a pure Lennard-Jones interaction

TABLE II. Bulk critical values for the density $\rho_c^* = \rho_c \sigma^3$, the temperature $T_c^* = k_B T_c / \epsilon$, and the chemical potential $\mu_c^* = \mu_c / \epsilon$ for various dipole strengths m^* of Stockmayer fluids obtained from the present density-functional theory by using a temperature-dependent hard-sphere diameter in the reference system.

m^*	ρ_c^*	T_c^*	μ_c^*
0.0	0.2757	1.3430	−4.6176
0.5	0.2758	1.3517	−4.6475
1.0	0.2774	1.4715	−5.0592
1.5	0.2826	1.8624	−6.4032
2.0	0.2906	2.5595	−8.7999

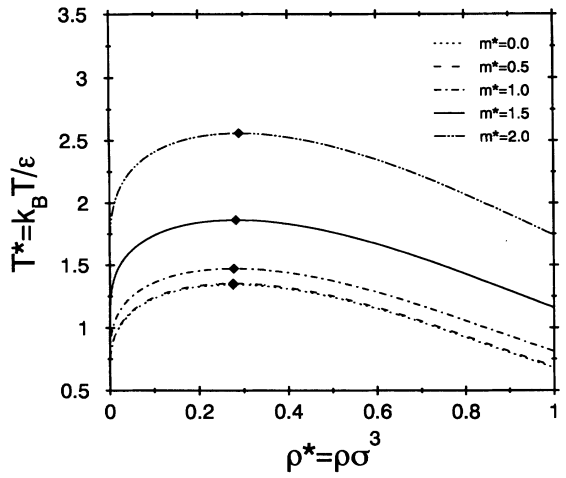

FIG. 5. Liquid-vapor phase diagrams of Stockmayer fluids with various dipole strengths m^* obtained from the present density-functional theory by using a temperature-dependent hard-sphere diameter in the reference system. The dots denote the critical points.

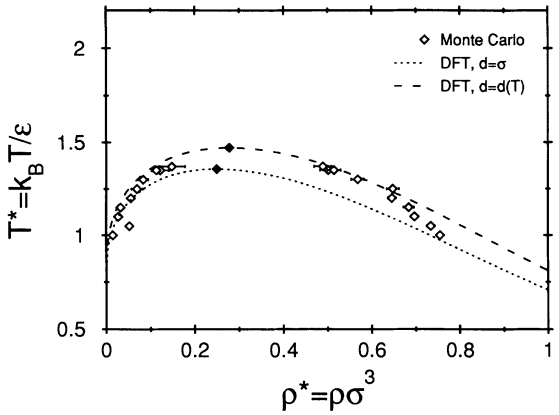

FIG. 6. Liquid-vapor phase diagram of a Stockmayer fluid with $m^*=1.0$ obtained by Monte Carlo methods [60] compared with the results for the same model by using either a constant or a temperature-dependent hard-sphere diameter for the reference system of the density-functional theory (DFT). The dots denote the critical points obtained from DFT for $d=\sigma$ and $d=d(T)$, respectively.

(see Fig. 3), there is a satisfactory agreement with that version of the DFT which uses a temperature-dependent hard-sphere diameter. The deviations for $\rho^*>0.7$ are caused by the low-density approximation for the pair distribution function entering the density-functional theory. On the other hand, one has to note that the Monte Carlo data do not allow one to reliably locate the critical point. Finally, we want to recall that Appendix A demonstrates the importance of retaining the full exponential function in Eq. (3.9) without expanding it.

IV. INTERFACIAL PROPERTIES

The knowledge of the bulk phase diagram obtained in Sec. III enables us to choose the chemical potential $\mu=\mu_0(T)$ such that, for a given temperature, the liquid and vapor phases coexist. For that choice of the thermodynamic variables we can impose vertical boundary conditions such that for $z\rightarrow+\infty$ one encounters the vapor phase and for $z\rightarrow-\infty$ the liquid phase. The lateral boundary conditions are chosen such that the mean position of the resulting interface of area A is fixed in the plane $z=0$. (For a discussion of the mean position of the free liquid-gas interface, see Ref. [13].) The system is translationally invariant in the x and y directions (see Fig. 1). Under these circumstances the total number density $\rho(z)$ is a function of z and the orientational profile $\alpha(\mathbf{r},\omega)=\alpha(z,\theta)=\bar{\alpha}(z,\theta)/2\pi$ depends only on z and the angle θ between the z axis and the dipole moment $\mathbf{m}$ of a molecule (see Fig. 1). For a system of size L in the vertical direction, the grand-canonical variational functional is given by [see Eq. (2.18)]

$$\frac{1}{A}\Omega[\{\rho(z),\bar{\alpha}(z,\theta)\},T,\mu]=\int_{-L/2}^{L/2}dz\, f_{\rm ref}^{\rm HS}(\rho(z),T)+\frac{1}{\beta}\int_{-L/2}^{L/2}dz\,\rho(z)\int_0^{\pi}d\theta\sin\theta\bar{\alpha}(z,\theta)\ln[2\bar{\alpha}(z,\theta)]$$
$$+\int_{-L/2}^{L/2}dz\,\rho(z)\int_0^{\pi}d\theta\sin\theta\bar{\alpha}(z,\theta)\phi_{\rm eff}(z,\theta)-\mu\int_{-L/2}^{L/2}dz\,\rho(z)\int_0^{\pi}d\theta\sin\theta\bar{\alpha}(z,\theta)$$
$$+\int_{-L/2}^{L/2}dz\,\kappa(z)\left[1-\int_0^{\pi}d\theta\sin\theta\bar{\alpha}(z,\theta)\right]. \tag{4.1}$$

The effective potential $\phi_{\rm eff}(z,\theta)$ contains the external potential $V_{\rm ext}(z,\theta)$ and the combined effect of those molecules acting on the plane $z=$const:

$$\phi_{\rm eff}(z,\theta)=V_{\rm ext}(z,\theta)-\frac{1}{2\beta}\int_{-\infty}^{+\infty}dx'\int_{-\infty}^{+\infty}dy'\int_{-L/2}^{L/2}dz'\Theta(R-\sigma)\rho(z')$$
$$\times\int_0^{\pi}d\theta'\sin\theta'\bar{\alpha}(z',\theta')\frac{1}{2\pi}\int_0^{2\pi}d\phi\frac{1}{2\pi}\int_0^{2\pi}d\phi'\tilde{f}(\mathbf{R},\theta,\phi,\theta',\phi'). \tag{4.2}$$

Here $\mathbf{R}=\mathbf{r}'-(0,0,z)=(x',y',z'-z)$, $\Theta(R-\sigma)$ is the Heaviside step function, and

$$\tilde{f}(\mathbf{R},\omega,\omega')=\mathbf{e}^{-\beta w_{ex}(\mathbf{R},\omega,\omega')}-1 \tag{4.3}$$

is the Mayer function of the excess intermolecular potential; ω and ω' denote the orientations of the molecules in a spatially fixed reference frame. Equation (4.1) can also easily be applied to the case of a wall-liquid or wall-vapor interface. In these cases V_{ext} acts as a substrate potential, so that $\rho(z\leq 0)=0=\kappa(z\leq 0)$. Furthermore, the boundary condition for $z\rightarrow+\infty$ must be adapted accordingly, and $L/2$ will be replaced by L. This is true as long as one disregards any lateral structure of the wall. Finally, one should note that Eq. (4.1) describes the so-called intrinsic interface structure as discussed in the Introduction.

A. Euler-Lagrange equations and rotationally invariant expansions

The equilibrium density and the orientational profile minimize Eq. (4.1) and are solutions of the following coupled Euler-Lagrange equations:

$$\mu=\mu_{HS}+\overline{\psi_{eff}}(z)\ , \tag{4.4}$$

$$\bar{\alpha}(z,\theta)=\tfrac{1}{2}(\mathbf{e}^{-\beta[\psi_{eff}(z,\theta)-\overline{\psi_{eff}}(z)]})\ . \tag{4.5}$$

$\psi_{eff}(z,\theta)$ is defined by the effective field introduced in Eq. (4.2),

$$\psi_{eff}(z,\theta)=2\phi_{eff}(z,\theta)-V_{ext}(z,\theta)\ , \tag{4.6}$$

and $\overline{\psi_{eff}}(z)$ is the angular average of the corresponding Boltzmann factor:

$$\overline{\psi_{eff}}(z)=-\frac{1}{\beta}\ln\tfrac{1}{2}\int_0^{\pi}d\theta\sin\theta\,\mathbf{e}^{-\beta\psi_{eff}(z,\theta)}\ . \tag{4.7}$$

$\mu_{HS}(z)$ is the local chemical potential of the reference system

$$\mu_{HS}(z)=\left.\frac{\partial f_{ref}^{HS}(\rho,T)}{\partial\rho}\right|_{\rho=\rho(z)}\ . \tag{4.8}$$

Now the angular dependence of ψ_{eff}, α, and V_{ext} is expressed in terms of Legendre polynomials $\mathcal{P}_l$:

$$\beta\psi_{eff}(z,\theta)=\sum_{l=0}^{\infty}q_l(z)\mathcal{P}_l(\cos\theta)\ , \tag{4.9}$$

$$\bar{\alpha}(z,\theta)=\sum_{l=0}^{\infty}\alpha_l(z)\mathcal{P}_l(\cos\theta)\ , \tag{4.10}$$

$$V_{ext}(z,\theta)=\sum_{l=0}^{\infty}v_l(z)\mathcal{P}_l(\cos\theta)\ . \tag{4.11}$$

In previous studies it was found that terms up to second order in this expansion provide the major contributions to the anisotropic orientation of the dipole molecules at the liquid-vapor interface [43]. In order to limit the computational efforts, we also constrain our analysis to terms up to second order in the Legendre polynomials. The treatment of higher-order terms would follow the same scheme. Inserting Eqs. (4.9), (4.10), and (4.11) into Eqs. (4.4) and (4.5) leads to the following set of coupled integral equations [due to $\mathcal{P}_0(x)=1$, $\mathcal{P}_1(x)=x$, $\mathcal{P}_2(x)=\frac{1}{2}(3x^2-1)$]:

$$\mu=\mu_{HS}(\rho(z))-\frac{1}{\beta}\left[-q_0(z)+\tfrac{1}{2}q_2(z)+\ln\left[\frac{1}{2}\int_{-1}^{1}dx\,e^{-q_1(z)x-(3/2)q_2(z)x^2}\right]\right],$$

$$\alpha_1(z)=\frac{3}{2}\frac{\int_{-1}^{1}dx\,xe^{-q_1(z)x-(3/2)q_2(z)x^2}}{\int_{-1}^{1}dx\,e^{-q_1(z)x-(3/2)q_2(z)x^2}}\ , \tag{4.12}$$

$$\alpha_2(z)=\frac{5}{4}\left[\frac{3\int_{-1}^{1}dx\,x^2e^{-q_1(z)x-(3/2)q_2(z)x^2}}{\int_{-1}^{1}dx\,e^{-q_1(z)x-(3/2)q_2(z)x^2}}-1\right].$$

The normalization condition on the orientational profile [see Eq. (2.2)] implies $\alpha_0(z)=\frac{1}{2}$.

According to Eqs. (4.2), (4.3), (4.6), (4.9), and (4.11), the coefficients $q_l(z)$ are determined by the coefficients $v_l(z)$ and $\alpha_l(z)$ and involve the Mayer function of the excess intermolecular potential, which depends on r_{12} and the solid angles ω, ω', and ω_{12}. These angles correspond to the orientations of the interacting dipoles and of the intermolecular axis $\mathbf{r}_{12}/r_{12}$, respectively, relative to a spatially fixed reference frame. In order to establish this relationship $\tilde{f}$ is expanded in terms of spherical harmonics $\mathcal{Y}_l^m$:

$$\tilde{f}(r_{12},\omega,\omega',\omega_{12})=\sum_{l_1,l_2,l=0}^{\infty}\sum_{m_1m_2m}{}'\,\bar{f}_{l_1l_2l}^{m_1m_2m}(r_{12})\mathcal{Y}_{l_1}^{m_1}(\omega)\times\mathcal{Y}_{l_2}^{m_2}(\omega')[\mathcal{Y}_l^m(\omega_{12})]^*\ , \tag{4.13}$$

where

$$\sum_{m_1,m_2,m}{}'=\sum_{m_1=-l_1}^{l_1}\sum_{m_2=-l_2}^{l_2}\sum_{m=-l}^{l}\ . \tag{4.14}$$

The intermolecular potential is invariant under arbitrary "passive" rotations in $\mathbb{R}^3$ of the spatially fixed reference frame, which is equivalent to an invariance under simultaneous "active" rotations of ω, ω', and ω_{12} relative to the spatially fixed coordinate frame. For fixed (l_1l_2l) up to a prefactor, there is the following unique combination of products of three spherical harmonics, which is invariant with respect to such rotations [61]:

$$\Phi_{\Lambda}(\omega,\omega',\omega_{12})=\sum_{m_1,m_2m}{}'\,C(l_1l_2l,m_1m_2m)\mathcal{Y}_{l_1}^{m_1}(\omega)\times\mathcal{Y}_{l_2}^{m_2}(\omega')[\mathcal{Y}_l^m(\omega_{12})]^*\ . \tag{4.15}$$

$C(l_1l_2l,m_1m_2m)$ are Clebsch-Gordan coefficients using the convention adopted by Rose [62] and $\Lambda=(l_1l_2l)\in\mathbb{N}_0^3$.

(This is a generalization of the addition theorem for products of two spherical harmonics, which states that $\sum'_m \mathcal{Y}_l^m(\omega)[\mathcal{Y}_l^m(\omega')]^*$ is invariant.) Therefore, the expansion coefficients in Eq. (4.13) must have the following special form:

$$\bar{f}_{l_1 l_2 l}^{m_1 m_2 m}(r_{12}) = C(l_1 l_2 l, m_1 m_2 m)\hat{f}_{l_1 l_2 l}(r_{12}) , \quad (4.16)$$

where the coefficients $\hat{f}$ are independent of the indices m_1, m_2, and m. The functions $\Phi_\Lambda(\omega,\omega',\omega_{12})$ form a complete set of basis functions for the expansion of such intermolecular potentials and functions thereof that exhibit the aforementioned rotational invariance [61]:

$$\tilde{f}(\mathbf{r}_{12},\omega,\omega') = \sum_\Lambda \hat{f}_\Lambda(r_{12})\Phi_\Lambda(\omega,\omega',\omega_{12}) . \quad (4.17)$$

They are orthogonal for each value of the solid angle ω_{12}:

$$\int_{S_2} d\omega \int_{S_2} d\omega' [\Phi_\Lambda(\omega,\omega',\omega_{12})]^* \Phi_{\Lambda'}(\omega,\omega',\omega_{12}) = \frac{2l+1}{4\pi}\delta_{\Lambda,\Lambda'} . \quad (4.18)$$

In comparison with Eq. (4.13), the particular form of the expansion in Eq. (4.17) offers the following advantages: (i) The rotational invariance determines the dependence of the expansion coefficients on the indices m_1, m_2, and m. (ii) The selection rules of the Clebsch-Gordan coefficients (they are zero unless one has $l=|l_1-l_2|,\ldots,l_1+l_2$ and $m_1+m_2=m$), various orthogonality, normalization, and sum-rule relations, and the particular symmetries of the dipole-dipole interaction potential enable one to eliminate many coefficients and to establish relations between the remaining ones which are nonzero [61]. (These details are presented in Appendix B.) (iii) Due to the rotational invariance, the expansion coefficients are the same for all possible orientations of the spatially fixed reference frame. Thus, by choosing a convenient reference frame, the explicit computation of the expansion coefficients can considerably be facilitated (see Appendix B).

According to Eq. (4.9) one has

$$q_l(z) = \beta\frac{2l+1}{2}\int_0^\pi d\theta \sin\theta \psi_{\text{eff}}(z,\theta)\mathcal{P}_l(\cos\theta) , \quad (4.19)$$

so that inserting Eqs. (4.2), (4.3), (4.6), (4.11), and (4.17) into Eq. (4.19) yields

$$q_{l_1}(z) = -\frac{1}{\sqrt{4\pi}}\int_{-L/2}^{L/2} dz\,\rho(z')\int_{|z'-z|}^\infty dr_{12} r_{12}\Theta(r_{12}-\sigma)\sum_{l_2,l=0}^\infty \alpha_{l_2}(z')\hat{f}_{l_1 l_2 l}(r_{12})\left[\frac{(2l_1+1)(2l+1)}{(2l_2+1)}\right]^{1/2} \times C(l_1 l_2 l,000)\mathcal{P}_l\left[\frac{z'-z}{r_{12}}\right] + \beta v_{l_1}(z) . \quad (4.20)$$

In order to proceed further, the coefficients $\hat{f}_\Lambda(r_{12})$ must be determined. This is done in Appendix B.

B. The free liquid-vapor interface

As mentioned before, the formulas in the previous subsection are applicable to various interfacial structures. Now we specialize them in order to study the free (i.e., without external fields) liquid-vapor interface. Since the coexisting l and g phases in the bulk are isotropic, this leads to the following boundary conditions:

$$\rho(z\to-\infty)=\rho_l,\quad \rho(z\to+\infty)=\rho_g , \qquad \bar{\alpha}(z\to-\infty,\theta)=\tfrac{1}{2},\quad \bar{\alpha}(z\to+\infty,\theta)=\tfrac{1}{2} . \quad (4.21)$$

In the absence of external fields, the effective potential ψ_{eff}, which enters the Euler-Lagrange equations Eqs. (4.4) and (4.5), is only due to intermolecular interactions:

$$\psi_{\text{eff}}(z,\theta;\{V_{\text{ext}}=0\}) = \sum_{l=0}^\infty p_l(z)\mathcal{P}_l(\cos\theta) , \quad (4.22)$$

with [see Eq. (4.6)]

$$p_l(z) = \frac{1}{\beta}q_l(z) - v_l(z) . \quad (4.23)$$

Since the dipolar interaction potential is invariant with respect to a rotation of 180° of both dipole moments, one has $\tilde{f}(\mathbf{r}_{12},\theta,\phi,\theta',\phi') = \tilde{f}(\mathbf{r}_{12},\pi-\theta,\phi\pm\pi,\pi-\theta',\phi'\pm\pi)$, where the upper (lower) signs hold for ϕ and ϕ', respectively, $\in(0,\pi)$ [$\in(\pi,2\pi)$]. In the absence of external fields this leads to [see Eqs. (4.2) and (4.5)]

$$\bar{\alpha}(z,\theta) = \bar{\alpha}(z,\pi-\theta),\quad \psi_{\text{eff}}(z,\theta) = \psi_{\text{eff}}(z,\pi-\theta) . \quad (4.24)$$

As a consequence $\alpha_l(z)=0=p_l(z)$ for odd values of l. Since $\alpha_0(z)=\frac{1}{2}$, within our approximation scheme (i.e., $l\le 2$) $\alpha_2(z)$ is the only remaining expansion coefficient for the orientational profile at the free liquid-vapor interface. This leads to the following closed set of integral equations:

$$\mu_{\text{HS}}(\rho(z)) = \mu - \left[p_0(z) - \tfrac{1}{2}p_2(z) - \frac{1}{\beta}\ln\int_0^1 dx\, e^{-(3/2)\beta p_2(z)x^2}\right] , \quad (4.25)$$

$$\alpha_2(z)=\frac{5}{4}\left[\frac{3\int_0^1 dx\, x^2 e^{-(3/2)\beta p_2(z)x^2}}{\int_0^1 dx\, e^{-(3/2)\beta p_2(z)x^2}}-1\right] . \tag{4.26}$$

The coefficients p_l are given by

$$p_{l_1}(z)=\int_{-\infty}^{\infty} dz' \rho(z') \sum_{l_2,l=0}^{\infty} \alpha_{l_2}(z') w_{l_1 l_2 l}(z'-z) , \tag{4.27}$$

with

$$w_{l_1 l_2 l}(y)=-\frac{1}{\beta}\frac{1}{\sqrt{4\pi}}\left[\frac{(2l_1+1)(2l+1)}{(2l_2+1)}\right]^{1/2} C(l_1 l_2 l,000) \times \int_{|y|}^{\infty} dr_{12} r_{12} \Theta(r_{12}-\sigma) \hat{f}_{l_1 l_2 l}(r_{12}) \mathcal{P}_l\left[\frac{y}{r_{12}}\right] . \tag{4.28}$$

Due to the symmetries of the dipolar interaction potential, the coefficients $\hat{f}_{l_1 l_2 l}(r_{12})$ vanish unless they fulfill the following conditions: l_1+l_2 even, l_1+l_2+l even, and $l\in\{|l_1-l_2|,\ldots,l_1+l_2\}$ (see Appendix B). Since $l_1,l_2\le 2$ the sum in Eq. (4.27) contains six terms: $(l_1 l_2 l)\in\{(000),(022),(202),(220),(222),(224)\}$. The expressions for the coefficients $\hat{f}_{l_1 l_2 l}(r_{12})$ are given in Eqs. (B27) and (B48)–(B51) of Appendix B. The corresponding values of the Clebsch-Gordan coefficients are $C(l_1 l_2 l,000)=1$, 1, 1, $1/\sqrt{5}$, $-\sqrt{2/7}$, and $3\sqrt{2/35}$, respectively. Although $\rho(z')$ approaches nonzero values for $|z'|\to\infty$, the z' integration can be extended to $\pm\infty$ because the second integral behaves asymptotically as $|z-z'|^{-4}$ for $|z-z'|\to\infty$. This is due to $\hat{f}_{l_1 l_2 l}(r_{12}\to\infty)\sim r_{12}^{-6}$ for all even values of l_1 and l_2 (see Appendix B). Note that due to Eq. (4.24) the index l_2 in Eq. (4.27) is even. Therefore the requirement that l_1+l_2 must be even (see Appendix B) leads to the conclusion that both l_1 and l_2 are even. Additionally, one has $\alpha_{l\neq 0}(|z|\to\infty)=0$, because $\bar{\alpha}(|z|\to\infty,\theta)=\frac{1}{2}=\alpha_0(z)$.

Thus the system of coupled integral equations, which determines the equilibrium number density profile $\rho(z)$ and the expansion coefficient $\alpha_2(z)$ of the orientational profile at the free liquid-vapor interface, consists of Eqs. (4.25) and (4.26) together with the following explicit expressions for the expansion coefficients of the effective potential $\psi_{\rm eff}(z,\theta)$:

$$p_0(z)=\int_{-\infty}^{\infty} dz' \rho(z')[\tfrac{1}{2} w_{000}(z'-z)+\alpha_2(z') w_{022}(z'-z)] , \tag{4.29}$$

$$p_2(z)=\int_{-\infty}^{\infty} dz' \rho(z')\{\tfrac{1}{2} w_{202}(z'-z)+\alpha_2(z') \times [w_{220}(z'-z)+w_{222}(z'-z) +w_{224}(z'-z)]\} . \tag{4.30}$$

C. Surface tension of the liquid-vapor interface

The solution of Eqs. (4.25), (4.26), (4.29), and (4.30) yields the intrinsic equilibrium density profile $\rho(z)$ and the orientational profile $\bar{\alpha}(z,\theta)$ of the liquid-vapor interface within our density-functional approach. In this subsection we want to present an explicit expression for the corresponding liquid-vapor surface tension σ_{lg} in terms of $\rho(z)$ and $\{\alpha_l(z)\}$. Inserting Eqs. (4.10) and (4.22) into Eq. (4.1) yields

$$\frac{1}{A}\Omega[\{\rho(z)\},\{\alpha_l(z)\},T,\mu]=\int_{-L/2}^{L/2} dz\, f_{\rm ref}^{\rm HS}(\rho(z),T)+\frac{1}{\beta}\int_{-L/2}^{L/2} dz\, \rho(z) \mathcal{S}(z) + \int_{-L/2}^{L/2} dz\, \rho(z) \sum_{l=0}^{\infty} \frac{1}{2l+1} \alpha_l(z) p_l(z)-\mu\int_{-L/2}^{L/2} dz\, \rho(z) , \tag{4.31}$$

where

$$\mathcal{S}(z)=\sum_{l=0}^{\infty} \alpha_l(z) \int_{-1}^{+1} dx \mathcal{P}_l(x) \ln\left[2\sum_{l'=0}^{\infty} \alpha_{l'}(z) \mathcal{P}_{l'}(x)\right] \tag{4.32}$$

stems from the entropy due to the orientational degrees of freedom of the hard spheres [see Eq. (2.25)]. Note that $\mathcal{S}(|z|\to\infty)=0$.

Equation (4.31) separates into the bulk contribution $\Omega_b(\rho,T,\mu)$ proportional to $V=AL$ [see Eqs. (3.2) and (3.3)] and into a surface contribution $\Omega_s[\{\rho(z)\},\{\alpha_l(z)\},T,\mu]$ proportional to A. The latter one contains the liquid-vacuum surface tension $\sigma_{l,\rm vac}=-\frac{1}{2}\rho_l^2\int_0^{\infty} dz\, t(z)$ and the vapor-vacuum surface tension $\sigma_{g,\rm vac}=-\frac{1}{2}\rho_g^2\int_0^{\infty} dz t(z)$ generated by the sharp cutoff at $z=-L$ and $+L$, respectively. (For the definition of the function $t(z)$ see, c.f., the definitions following Eq. (4.37). The expressions for the bulk-vacuum surface tensions are identical in their *form* with the corresponding ones for an isotropic fluid given in Eq. (2.7) in Ref. [63].) Therefore the liquid-vapor surface tension is given by

$$\sigma_{l,g}=\lim_{L\to\infty}\left[\frac{\Omega}{A}-\frac{\Omega_b}{A}\right]-\sigma_{l,\rm vac}-\sigma_{g,\rm vac} . \tag{4.33}$$

Due to Eq. (4.21) the density profile $\rho(z)=\rho_{\rm SK}(z)+\delta\rho(z)$

can be decomposed into a sharp-kink (SK) contribution $\rho_{\rm SK}(z)=\rho_l-\Delta\rho\Theta(z)$, $\Delta\rho=\rho_l-\rho_g$, and a contribution $\delta\rho(z)$ which vanishes for $|z|\to\infty$; $\alpha_{l\neq 0}(|z|\to\infty)=0$. A rearrangement in Eqs. (4.31) and (4.33) allows us to express $\sigma_{l,g}$ in terms of $\delta\rho(z)$ and $\alpha_l(z)$. One obtains three distinct contributions,

$$\sigma_{l,g}=\sigma_{l,g}^{(\rho)}+\sigma_{l,g}^{(\mathcal{S})}+\sum_{\Lambda[\neq(000)]}\sigma_{l,g}^{(\Lambda)}\ , \tag{4.34}$$

which are given by the density profile alone, by $\mathcal{S}(z)$, and by the deviation from isotropy, where $\Lambda=(l_1l_2l)\in\mathbb{N}^3$, respectively:

$$\sigma_{l,g}^{(\rho)}=\int_{-\infty}^{\infty}dz\,[f_{\rm ref}^{\rm HS}(\rho(z),T)-f_{\rm ref}^{\rm HS}(\rho_{\rm SK}(z),T)]+\tfrac{1}{2}\int_{-\infty}^{\infty}dz\int_{-\infty}^{\infty}dz'\delta\rho(z)\delta\rho(z')w(z-z')$$
$$+\int_{-\infty}^{\infty}dz[w_0\rho_{\rm SK}(z)-\mu_0(T)]\delta\rho(z)+\Delta\rho\int_{-\infty}^{\infty}dz(\mathrm{sgn}z)\,t(|z|)\delta\rho(z)-\tfrac{1}{2}(\Delta\rho)^2\int_0^{\infty}dz\,t(z)\ , \tag{4.35}$$

$$\sigma_{l,g}^{(S)}=\frac{1}{\beta}\left[\int_{-\infty}^{\infty}dz\,\rho_{\rm SK}(z)\mathcal{S}(z)+\int_{-\infty}^{\infty}dz\,\delta\rho(z)\mathcal{S}(z)\right]\ , \tag{4.36}$$

and

$$\sigma_{l,g}^{(\Lambda)}=\int_{-\infty}^{\infty}dz\,[\rho_{\rm SK}(z)]^2\alpha_{l_1}(z)[t_\Lambda^{(0)}(z)-t_\Lambda^{(1)}(z)]+\rho_l\rho_g\left[\int_{-\infty}^{0}dz\,\alpha_{l_1}(z)\,t_\Lambda^{(+)}(|z|,z)+\int_0^{\infty}dz\,\alpha_{l_1}(z)\,t_\Lambda^{(-)}(|z|,z)\right]$$
$$+\int_{-\infty}^{\infty}dz\int_{-\infty}^{\infty}dz'\delta\rho(z)\delta\rho(z')\alpha_{l_1}(z)\alpha_{l_2}(z')w_\Lambda(z'-z)$$
$$+2\int_{-\infty}^{\infty}dz\,\rho_{\rm SK}(z)\alpha_{l_1}(z)[t_\Lambda^{(0)}(z)-t_\Lambda^{(1)}(z)]\delta\rho(z)+2\int_{-\infty}^{\infty}dz\,\rho_{\rm SK}(-z)\alpha_{l_1}(z)t_\Lambda^{(1)}(z)\delta\rho(z)\ . \tag{4.37}$$

In Eq. (4.35), $w(y)=\frac{1}{2}w_{000}(y)$ [see Eq. (4.28) for the definition of $w_\Lambda(y)$], $t(z)=\int_z^{\infty}dy\,w(y)$, and $w_0=2t(0)$. In Eq. (4.37) we have introduced the following abbreviations:

$$t_\Lambda^{(\pm)}(a,b)=\int_a^{\infty}dy\,\alpha_{l_2}(b\pm y)w_\Lambda(y)\ ,$$
$$t_\Lambda^{(0)}(z)=t_\Lambda^{(+)}(0,z)+t_\Lambda^{(-)}(0,z)\ , \tag{4.38}$$
$$t_\Lambda^{(1)}(z)=t_\Lambda^{(+)}(|z|,z)-[t_\Lambda^{(+)}(|z|,z)-t_\Lambda^{(-)}(|z|,z)]\Theta(z)\ .$$

The density profile is expected to exhibit van der Waals tails, i.e., $\delta\rho(|z|\to\infty)\sim z^{-3}$, as in an isotropic van der Waals fluid (see Ref. [13]). For even values of l_1, l_2, and l—and only such combinations enter Eqs. (4.34) and (4.37)—one has $w_\Lambda(|y|\to\infty)\sim|y|^{-4}$, so that for large values of z the functions $t_\Lambda^{(\pm)}(|z|,z)$, $t_\Lambda^{(0)}(z)$, and $t_\Lambda^{(1)}(z)$ vanish at least proportional to $|z|^{-3}$. Therefore the infinite integrals in Eqs. (4.35) and (4.37) do exist. The convergence of the first integral in Eq. (4.36) requires that $\alpha_{l\neq 0}(|z|\to\infty)\sim|z|^{-(1+\epsilon)}$ with $\epsilon>0$.

Equation (4.34) yields a natural decomposition of the total surface tension into an isotropic part and various contributions due to the anisotropy generated by the presence of the interface. If the interfacial structure were isotropic, i.e., $\alpha_{l\neq 0}=0$, one would have $\sigma_{l,g}=\sigma_{l,g}^{(\rho)}$.

Furthermore, the expression for $\sigma_{l,g}^{(\rho)}$ in Eq. (4.35) is identical in its form, with the known formula for an isotropic fluid given in Eq. (2) in Ref. [64]. Note that Eq. (2) in Ref. [64] has been derived for a density-functional theory of an isotropic van der Waals fluid with $g^{(2)}=1$. Thus Eq. (4.35) generalizes this result for the case that instead of $g^{(2)}=1$, the low-density approximation [see Eq. (2.15)] is applied. Accordingly, for *isotropic* interactions the functions $w(y)=(2\pi/\beta)\int_{|y|}^{\infty}dr\,r\Theta(r-\sigma)\times[1-e^{-\beta w_{\rm LJ}(r)}]$ and $t(z)$ represent the generalized versions of the corresponding ones defined in Refs. [13] and [64], to which they reduce in the limit $\beta\to\infty$ if one takes into account that we apply the Barker-Henderson approach [see Eq. (2.19)] compared with the Weeks-Chandler-Andersen approach used in Refs. [13] and [64].

$\sigma_{l,g}^{(\mathcal{S})}$ is that contribution to the surface tension which stems from the orientational degrees of freedom of the hard-sphere reference system [see Eq. (2.25)]. Finally, $\sigma_{l,g}^{(\Lambda)}$ are those contributions which are genuinely due to the preferential orientational order at the interface. In our present approximation scheme, i.e., $\alpha_{l>2}=0$, only the following terms arise: $\Lambda=(l_1l_2l)\in\{(022),(202),(220),(222),(224)\}$. [The term $\Lambda=(000)$ is already included in Eq. (4.35).] Accordingly, in $\mathcal{S}(z)$ only terms with $l=0,2$ and $l'=0,2$ are taken into account. Thus inserting the solutions for $\rho(z)$ and $\alpha_2(z)$ together with $a_0(z)=\frac{1}{2}$ obtained from Eqs. (4.25), (4.26), (4.29), and (4.30) yields the equilibrium liquid-vapor surface tension. It is reassuring that the functional derivative of Eqs. (4.35)–(4.37) with respect to $\rho(z)$ and $\alpha_2(z)$ leads to the correct Euler-Lagrange equations (4.25) and (4.26).

V. APPLICATION TO NEMATIC FLUIDS

As mentioned in Sec. II, the DFT can be applied to molecular fluids with more general anisotropic intermolecular interaction potentials than the dipole-dipole interaction potential discussed above. In this respect, liquid crystals are of particular interest, since they exhibit various degrees of spatial and orientational order [65]; e.g., in the nematic phase there is long-range orientational order but no spatial order. In view of the previous section, the natural question arises as to what kind of prefer-

ential ordering is generated at the liquid-vapor interface of such liquids above the nematic phase-transition temperature.

Without attempting to give an overview of this wide field of research, it seems fair to say that there are basically two lines of attack in order to resolve such structures on the basis of statistical mechanics. The first one emphasizes the highly anisotropic shapes of the molecules and the corresponding steric interactions. Within this approach, the free-energy functional is taken to be the sum of the free-energy functional of an ideal gas and the excess free-energy functional

$$\mathcal{F}_{\rm ex}[\{\hat{\rho}(\mathbf{r},\omega)\},T]=-\frac{1}{2\beta}\int\int d^3r\,d^3r'd\omega\,d\omega' \times\tilde{f}(\mathbf{r}_{12},\omega,\omega') \times\hat{\rho}(\mathbf{r},\omega)\hat{\rho}(\mathbf{r}',\omega')\ , \tag{5.1}$$

where the Mayer function $\tilde{f}$ is taken to be -1 if two molecules overlap, and 0 otherwise. Here, long-range attractive interactions are completely ignored (see, e.g., Refs. [66–68]).

In the second line of attack, one adopts the opposite point of view. There the anisotropic part of the steric interactions is ignored, i.e., the reference system consists of hard spheres, whereas the anisotropy is supported by a long-range attractive interaction potential (see, e.g., Ref. [19]):

$$w_{\rm nem}(\mathbf{r}_{12},\omega,\omega')=-A\left[\frac{\sigma}{r_{12}}\right]^6-B\left[\frac{\sigma}{r_{12}}\right]^6\mathcal{P}_2(\hat{\mathbf{n}}(\omega)\hat{\mathbf{n}}(\omega')) +C\left[\frac{\sigma}{r_{12}}\right]^6[\mathcal{P}_2(\hat{\mathbf{n}}(\omega)\hat{\mathbf{r}}_{12}) +\mathcal{P}_2(\hat{\mathbf{n}}(\omega')\hat{\mathbf{r}}_{12})]\ , \tag{5.2}$$

where A, B, and C are suitably chosen energy parameters, $\hat{\mathbf{r}}_{12}=\mathbf{r}_{12}/r_{12}$, and $\hat{\mathbf{n}}(\omega)$ and $\hat{\mathbf{n}}(\omega')$ are the unit vectors of the directions of the two interacting molecules. (Note that for most molecules that form liquid crystals their heads are different from their tails so that for the corresponding direction $\hat{\mathbf{n}}(\omega)$ one has $\omega\in S_2$. However, all energy differences associated with this distinction are usually ignored.) Since $\mathcal{P}_2$ is the second Legendre polynomial, $w_{\rm nem}$ is invariant if the direction of *one* molecule is reversed. Thus $w_{\rm nem}$ exhibits more symmetry properties than the dipole-dipole interaction potential

$$w_{\rm dip}(\mathbf{r}_{12},\omega,\omega')=-\frac{m^2}{r_{12}^3}[3\mathcal{P}_1(\hat{\mathbf{m}}(\omega)\hat{\mathbf{r}}_{12})\mathcal{P}_1(\hat{\mathbf{m}}(\omega')\hat{\mathbf{r}}_{12}) -\mathcal{P}_1(\hat{\mathbf{m}}(\omega)\hat{\mathbf{m}}(\omega'))]\ .$$

Whereas the first approach may be particularly suitable for long molecules, the second one may be more appropriate for shorter molecules. Obviously, one would like to combine both in order to obtain reliable results.

Since the second approach fits into the general scheme described in the previous sections, we want to comment on that. It turns out that *all* formulas and statements in Secs. II–IV remain valid if $w_{\rm ex}(\mathbf{r},\mathbf{r}',\omega,\omega')$ is replaced by $w_{\rm nem}(\mathbf{r}_{12},\omega,\omega')$ instead of $w_{\rm SI}(\mathbf{r}_{12},\omega,\omega')$. (The subscript SI denotes the Stockmayer-interaction potential [see Eq. (2.23)].) The difference between the Stockmayer fluid and the nematic fluid is only due to different explicit expressions for the expansion coefficients $\hat{f}_{l_1l_2l}(r_{12})$ for the Mayer function [see Eqs. (4.17), (4.27), and (4.28)]. Both $\hat{f}^{\rm SI}_{\Lambda}(r_{12})$ and $\hat{f}^{\rm nem}_{\Lambda}(r_{12})$ are characterized by the same set $\Lambda=(l_1l_2l)\in\{(000),(022),(202),(220),(222),(224)\}$ if one considers in both cases only the second expansion coefficient $\alpha_2(z)$ for the orientational profile at the liquid-vapor interface. (Also for nematic fluids one has $\alpha_0=\frac{1}{2}$ and $\alpha_l=0$ for odd l.) For more details see Appendix C.

The formulas quoted above are valid for the density-functional theory in which the pair distribution function $g^{(2)}$ is approximated by its low-density limit in the bulk [see Eqs. (2.11) and (2.15)]. In an even cruder approximation one would chose $g^{(2)}=1$, which leads to a null result in the case of purely multipolar interaction potentials [see Eq. (2.14)] but to a nontrivial expression in the case of nematic liquids [19]:

$$\mathcal{F}_{\rm ex}[\{\hat{\rho}(\mathbf{r},\omega)\},T]=\tfrac{1}{2}\int\int d^3r\,d^3r'd\omega d\omega' w_{\rm nem}(\mathbf{r}_{12},\omega,\omega') \times\hat{\rho}(\mathbf{r},\omega)\hat{\rho}(\mathbf{r}',\omega')\ . \tag{5.3}$$

The density-functional theory based on Eq. (5.3) is even capable of predicting a bulk phase diagram that contains a vapor phase and both isotropic and nematic liquid phases [19]. Therefore, there is a qualitative difference of the DFT with $g^{(2)}=1$ used for dipolar or nematic fluids. However, our remarks above show that this qualitative difference in description of these two kinds of complex fluids disappears as soon as one uses the DFT with $g^{(2)}=e^{-\beta w_{\rm ex}}$. As pointed out within this latter approach, it becomes apparent that there are important similarities between the structural properties of liquid-vapor interfaces of dipolar fluids and nematic fluids. Nonetheless, there will certainly be interesting quantitative differences that should be revealed by numerical solutions of the density and orientational profiles.

Finally, from our approach it also follows that either external anisotropic fields or the confinement due to walls will destroy this similarity of the two systems, because they generate nonzero expansion coefficients $\hat{f}^{\rm SI}_{110}(r_{12})$ $\hat{f}^{\rm SI}_{112}(r_{12})$, which are missing in nematic liquids.

VI. SUMMARY

The following main results have been obtained:

(i) We have formulated a density-functional theory for a microscopic description of inhomogeneous, one-component molecular fluids [see Sec. II A and Eqs. (2.18), (2.24), and (2.25)]. In particular, we focus on systems governed by a combination of dipolar and isotropic dispersion forces and model them by Stockmayer potentials [see Sec. II B and Eq. (2.23)].

(ii) The bulk properties of these Stockmayer fluids follow from an effective isotropic interaction potential [see Sec. III A, Fig. 2, and Eqs. (3.6) and (3.11)].

(iii) We have calculated the bulk phase diagrams of Stockmayer fluids for various strengths of the permanent

dipole moments (see Sec. III B Figs. 4 and 5, and Tables I and II). We find good agreement with simulation data (see Figs. 3 and 6).

(iv) In comparison with a previous DFT for the same system, which was based on more approximations than the present one, we have achieved an improvement of 10–18 % in locating the phase boundaries in the phase diagram (see Appendix A and Fig. 7). Our approach allows one to treat systems with even strong dipolar forces.

(v) Our DFT enables us to determine density and orientational profiles at liquid-vapor, wall-liquid, and wall-vapor interfaces of molecular fluids. It is also capable of describing wetting phenomena. The general analytical expressions for these profiles are given in Sec. IV A [see Eqs. (4.12) and (4.20)].

(vi) As far as the leading contribution to the anisotropic part of the orientational profile is concerned, the intrinsic structure of the free-liquid interface of Stockmayer fluids is given by two coupled nonlinear integral equations for the density and the orientational profile [see Sec. IV B and Eqs. (4.25), (4.26), (4.29), and (4.30)]. The derivation of these equations and the explicit formulas are presented in Appendix B [see Eqs. (B27) and (B48)–(B51) entering Eq. (4.27) and thus Eqs. (4.29) and (4.30)].

(vii) These results show that the density profile influences the orientational profile and vice versa. Therefore, unlike numerous other studies, we find that the orientational profile does influence the density profile.

(viii) Our approach avoids truncations that were used in previous studies of these systems. Thus we can analyze the influence of strong dipolar forces on interfacial structures.

(ix) The surface tension of the liquid-vapor interface can be separated into an isotropic and into several anisotropic contributions [see Eqs.(4.34)–(4.37)]. Their physical relevance is discussed in Sec. VI C.

(x) According to Appendix C, our analytic results can be translated to nematic fluids. As shown in Sec. V, there is a qualitative similarity in the structures of the liquid-vapor interfaces in dipolar and nematic fluids, respectively.

ACKNOWLEDGMENTS

We would like to thank M. Schick for helpful discussions and W. Koch and A. Haase for their assistance with computer programs.

APPENDIX A: COMPARISON BETWEEN THE TRUNCATED AND FULL VERSIONS OF THE DENSITY-FUNCTIONAL THEORY

In a recent publication, Teixeira and Telo da Gama [14] studied the orientational order at the free liquid-gas interface of a dipolar fluid by using the same DFT as we use [see Eq. (2.18)]. However, different from our approach, they expanded the term $\exp(-\beta w_{ex})$ entering Eq. (2.18) in a series that they truncated after the second term. Since our approach of keeping the full exponential function requires significantly more analytic and numerical efforts, one would like to check whether these additional efforts are necessary. Certainly, the difference between the two results will become small for higher temperatures. For that reason we compare the bulk phase diagrams predicted by the truncated theory and our full theory, respectively, in particular close to T_c where the truncated version works best.

In order to be able to compare these results, we have repeated our calculations for the following model of dipolar fluids adopted by Teixeira and Telo da Gama, which differs from that we discussed in Sec. II B:

$$w_{ref}(r_{12})=\begin{cases}+\infty, & r_{12}\le\sigma\\ 0, & r_{12}>\sigma\end{cases},$$

$$w_{ex}(\mathbf{r}_{12},\omega,\omega')=\begin{cases}0, & r_{12}\le\sigma\\ -4\epsilon\left[\dfrac{\sigma}{r_{12}}\right]^6+w_{dip}(\mathbf{r}_{12},\omega,\omega'), & r_{12}>\sigma\end{cases}.$$

In the truncated approach Eq. (3.3) is replaced by

$$U(T)=4\pi\int_\sigma^\infty dr_{12}r_{12}^2\left[\langle w_{ex}(\mathbf{r}_{12},\omega,\omega')-\frac{\beta}{2}w_{ex}^2(\mathbf{r}_{12},\omega,\omega')\rangle_{\omega\omega'}\right]$$

$$=4\pi\int_\sigma^\infty dr_{12}r_{12}^2\left[\hat{w}_{LJ}(r_{12})-\frac{\beta}{2}\hat{w}_{LJ}^2(r_{12})+\frac{\beta}{2}\langle w_{dip}^2(\mathbf{r}_{12},\omega,\omega')\rangle_{\omega\omega'}\right].$$

where $\hat{w}_{LJ}^2(r_{12}\ge\sigma)=-4\epsilon(\sigma/r_{12})^6$. The angular average of odd powers of the dipole-dipole interaction potential vanishes.

In Fig. 7 for four reduced dipole strengths $m^*=(m^2/\sigma^3\epsilon)^{1/2}$ the bulk phase diagrams predicted by the truncated theory and the full theory are compared. As displayed in Table III, the truncated version underestimates the value of T_c by 10% in the absence of dipolar interactions; this discrepancy increases to 18% for $m^*=2$. Here we want to emphasize that this increase of the value of T_c in the full theory is not only due to retain-

TABLE III. Critical temperature $T_c^*=k_BT_c/\epsilon$ for various reduced dipole strengths m^* according to the truncated version of the density-functional theory used in Ref. [14] compared with the full theory.

	T_c^*	
m^*	Truncated version	Full theory
0.0	2.0098	2.2048
1.0	2.0590	2.2848
1.5	2.2420	2.5615
2.0	2.6488	3.1152

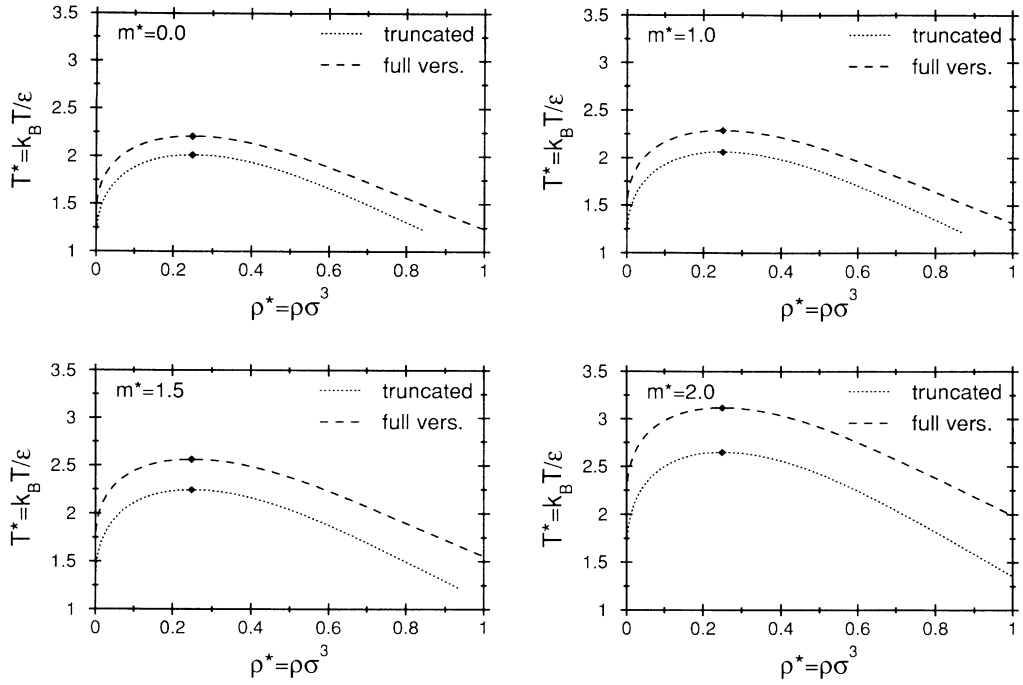

FIG. 7. Bulk phase diagrams for various reduced dipole strengths m^* obtained from the truncated version of the density-functional theory used in Ref. [14] compared with our full theory. Since in Ref. [14] no temperature-dependent hard-sphere diameter was used, this comparison corresponds to $d=\sigma$. The dots indicate the critical points.

ing terms that contain arbitrarily high powers of w_{LJ} or w_{dip}^2, but is also due to cross terms that involve powers of w_{LJ} and even powers of w_{dip}^2. In the spatially inhomogeneous case of interfacial structures, these cross terms enhance the coupling between positional and orientational degrees of freedom compared with that retained in the truncated version.

Since the results shown in Fig. 6 encourage us to strive for quantitatively reliable predictions, we feel that it is worthwhile to work out the full theory in spite of its technical challenges. Finally, we want to remark that in Ref. [14] the dependence of the critical density on the strength of the dipole moment (see Table II) was not taken into account. However, this is only due to the temperature-dependent hard-sphere diameter we are using. As can be inferred from Eqs. (3.2) and (3.16), the value of ρ_c is the same for the full and truncated versions of the density-functional theory.

APPENDIX B: DETERMINATION OF THE EXPANSION COEFFICIENTS OF THE MAYER FUNCTION

According to Eqs. (4.27) and (4.28), solving the set of integral equations (4.25) and (4.26) requires to determine the expansion coefficients $\hat{f}_\Lambda(r_{12})$ of the Mayer function $\tilde{f}$ of the excess intermolecular potential. They are given by [see Eqs. (4.15), (4.17), and (4.18)]

$$\hat{f}_\Lambda(r_{12})=\frac{4\pi}{2l+1}\int_{S_2}d\omega\int_{S_2}d\omega'\tilde{f}(r_{12},\omega,\omega',\omega_{12})\times\Phi_\Lambda^*(\omega,\omega',\omega_{12})\ . \tag{B1}$$

According to Eq. (B1), the left-hand side is independent of ω_{12} so that the right-hand side can be evaluated for the convenient value $\omega_{12}=(\theta_{12},\phi_{12})=(0,0)$. With $\mathcal{Y}_l^m(0,0)=\sqrt{2l+1/4\pi}\,\delta_{m,0}$ one obtains from Eq. (B1) ($\bar{m}\equiv -m$)

$$\hat{f}_\Lambda(r_{12})=\left[\frac{4\pi}{2l+1}\right]^{1/2}\sum_m C(l_1l_2l,m\bar{m}0)\int_{S_2}d\omega\int_{S_2}d\omega'\tilde{f}(r_{12},\omega,\omega',\omega_{12}=0)[\mathcal{Y}_{l_1}^m(\omega)]^*[\mathcal{Y}_{l_2}^{\bar{m}}(\omega')]^*\ . \tag{B2}$$

Here and in the following the sum over m extends from $-\min(l_1,l_2)$ to $+\min(l_1,l_2)$. Thus the coefficients $\hat{f}_\Lambda(r_{12})$ can be expressed in terms of reduced coefficients $f_{l_1l_2m}(r_{12})$,

$$\hat{f}_\Lambda(r_{12})=\left[\frac{4\pi}{2l+1}\right]^{1/2}\sum_m C(l_1l_2l,m\bar{m}0)f_{l_1l_2m}(r_{12})\ , \tag{B3}$$

with

$$f_{l_1 l_2 m}(r_{12}) = \int_{S_2} d\omega \int_{S_2} d\omega' \tilde{f}(r_{12},\omega,\omega',\omega_{12}=0) \times [\mathcal{Y}^m_{l_1}(\omega)]^* [\mathcal{Y}^{\bar{m}}_{l_2}(\omega')]^* , \quad \text{(B4)}$$

which correspond to an expansion of the Mayer function of the excess potential in an intermolecular coordinate system, i.e., the intermolecular vector $\mathbf{r}_{12}$ points into the z direction of the spatially fixed reference frame.

1. Symmetries

The Mayer function $\tilde{f}$, which determines the expansion coefficients $\hat{f}_\Lambda$ and $f_{l_1 l_2 m}$, respectively, exhibits the same symmetries as the corresponding excess intermolecular potential. The particular symmetries of the dipole-dipole interaction potential considerably reduce the number of independent coefficients:

(i) w_{ex} is invariant with respect to any rotation of the spatially fixed reference frame, so that $\tilde{f}(r_{12},\omega,\omega',\omega_{12})$ can be expanded in terms of the rotationally invariant functions $\Phi_{l_1 l_2 l}(\omega,\omega',\omega_{12})$ [see Eqs. (4.15) and (4.17)]. Since the Clebsch-Gordan coefficients $C(l_1 l_2 l, m_1 m_2 m)$ vanish unless $l \in \{|l_1-l_2|, |l_1-l_2|+1, \ldots, l_1+l_2-1, l_1+l_2\}$, the coefficients $\hat{f}_{l_1 l_2 l}(r_{12})$ are nonzero only if l_1, l_2, and l fulfill this selection rule, for which we use the short notation $l_1+l_2+l=\Delta$.

(ii) The dipole-dipole interaction potential is invariant with respect to an inversion of all coordinates: $\omega \to -\omega$, $\omega' \to -\omega'$, $\omega_{12} \to -\omega_{12}$, with $-\omega = (\pi-\theta, \phi+\pi)$ for $\phi \in (0,\pi)$ and $-\omega = (\pi-\theta, \phi-\pi)$ for $\phi \in (\pi, 2\pi)$. Due to $\mathcal{Y}^m_l(-\omega) = (-1)^l \mathcal{Y}^m_l(\omega)$ one has $\Phi_\Lambda(-\omega,-\omega',-\omega_{12}) = (-1)^{l_1+l_2+l} \Phi_\Lambda(\omega,\omega',\omega_{12})$, so that the above symmetry leads to $\hat{f}_\Lambda(r_{12}) = (-1)^{l_1+l_2+l} \hat{f}_\Lambda(r_{12})$, i.e., the coefficients $\hat{f}_\Lambda(r_{12})$ are nonzero only if l_1+l_2+l is even.

(iii) Since the Clebsch-Gordan coefficients are real and fulfill the relation $C(l_1 l_2 l, m_1 m_2 m) = (-1)^{l_1+l_2+l} C(l_1 l_2 l, \bar{m}_1 \bar{m}_2 \bar{m})$, the functions $\Phi_\Lambda(\omega,\omega',\omega_{12})$ are real for l_1+l_2+l even. Due to (ii) and Eq. (B1), the coefficients $\hat{f}_\Lambda(r_{12})$ are real. This is also true for the reduced coefficients $f_{l_1 l_2 m}(r_{12}) = \sum_{l=0}^{\infty} \sqrt{2l+1/4\pi}\, C(l_1 l_2 l, m\bar{m}0) \hat{f}_{l_1 l_2 l}(r_{12})$.

(iv) By definition, $f^*_{l_1 l_2 m}(r_{12}) = f_{l_1 l_2 \bar{m}}(r_{12})$ [see Eq. (4.16)], so that (iii) yields $f_{l_1 l_2 m}(r_{12}) = f_{l_1 l_2 \bar{m}}(r_{12})$.

(v) Since an exchange of the two interacting molecules ($\omega \to \omega', \omega' \to \omega, \omega_{12} \to -\omega_{12}$) does not change w_{ex}, one has $\hat{f}_{l_1 l_2 l}(r_{12}) = (-1)^l \hat{f}_{l_2 l_1 l}(r_{12}) = (-1)^{l_1+l_2} \hat{f}_{l_2 l_1 l}(r_{12})$. Due to $C(l_1 l_2 l, m\bar{m}0) = C(l_2 l_1 l, m\bar{m}0)$ one also has $f_{l_1 l_2 m}(r_{12}) = (-1)^{l_1+l_2} f_{l_2 l_1 \bar{m}}(r_{12})$ [see (iii)].

(vi) The dipole-dipole interaction is invariant under the exchange of the orientation of the two molecules ($\omega \to \omega', \omega' \to \omega, \omega_{12} \to \omega_{12}$). Therefore, Eq. (4.16) yields $f_{l_1 l_2 m}(r_{12}) = f_{l_2 l_1 \bar{m}}(r_{12})$. The result in (iv) implies $f_{l_1 l_2 m}(r_{12}) = f_{l_2 l_1 m}(r_{12})$. According to (v), this means that l_1+l_2 is even in both $f_{l_1 l_2 m}(r_{12})$ and $\hat{f}_{l_1 l_2 l}(r_{12})$.

2. Recurrence relations

In order to evaluate the reduced coefficients f [see Eq. (B4)] we expand the dipole-dipole interaction potential in the exponent of the Mayer function [see Eq. (4.3)] in terms of rotational invariants, as well:

$$\beta w_{dip}(r_{12},\omega,\omega',\omega_{12}) = \sum_\Lambda \hat{u}_\Lambda(r_{12}) \Phi_\Lambda(\omega,\omega',\omega_{12}) . \quad \text{(B5)}$$

Here, only those expansion coefficients $\hat{u}_{l_1 l_2 l}(r_{12})$ that correspond to $l_1=l_2=1$ are nonzero [42].

In the intermolecular reference frame, the reduced expansion coefficients $u_{l_1 l_2 m}(r_{12})$ can be inferred from [see Eq. (B2)] ($u_m \equiv u_{11m}$)

$$\beta w_{dip}(r_{12},\omega,\omega',\omega_{12}=0) = \sum_{m=-1}^{1} u_m(r_{12}) \mathcal{Y}^m_1(\omega) \mathcal{Y}^{\bar{m}}_1(\omega') , \quad \text{(B6)}$$

where the coefficients $u_m(r_{12})$ are given by

$$u_1(r_{12}) = u_{-1}(r_{12}) = \tfrac{1}{2} u_0(r_{12}) = -\frac{4\pi}{3} \frac{\beta m^2}{r_{12}^3} = -\frac{4\pi}{3} Z . \quad \text{(B7)}$$

With the expansion in Eq. (B6), the reduced coefficients f have the following explicit form:

$$f_{l_1 l_2 m} = \int_{S_2} d\omega \int_{S_2} d\omega' [\mathcal{Y}^m_{l_1}(\omega)]^* [\mathcal{Y}^{\bar{m}}_{l_2}(\omega')]^* \left[-1 + e^{-\beta w_{LJ}(r_{12})} \exp\left[-\sum_{m'=-1}^{1} u_{m'}(r_{12}) \mathcal{Y}^{m'}_1(\omega) \mathcal{Y}^{\bar{m}'}_1(\omega') \right] \right] . \quad \text{(B8)}$$

Since

$$\int_{S_2} d\omega \int_{S_2} d\omega' [\mathcal{Y}^m_{l_1}(\omega)]^* [\mathcal{Y}^{\bar{m}}_{l_2}(\omega')]^* = 4\pi \delta_{l_1 0} \delta_{l_2 0} \delta_{m0} ,$$

the first term in the curly brackets in Eq. (B8) contributes *only* to $f_{000}(r_{12})$ and therefore it gives rise to a contribution $\hat{f}^{(-1)}_{000}(r_{12})$ of $\hat{f}_{000}(r_{12})$ [see Eq. (B3)]:

$$\hat{f}^{-1}_{000}(r_{12}) = \sqrt{4\pi}\, C(000,000)(-4\pi) = -(4\pi)^{3/2} . \quad \text{(B9)}$$

Thus in the following calculations for $f_{l_1 l_2 m}(r_{12})$ we can omit the first term in the curly brackets in Eq. (B8) provided that the term $-(4\pi)^{3/2}$ is added to the expression corresponding to $\hat{f}_{000}(r_{12})$.

In the next step we calculate the partial derivative of $f_{l_1 l_2 m}(r_{12})$ with respect to the coefficients $u_m(r_{12})$ defined in Eqs. (B6) and (B7):

$$\frac{\partial f_{l_1 l_2 m}(r_{12})}{\partial u_{m''}(r_{12})} = -\int_{S_2} d\omega \int_{S_2} d\omega' \mathcal{Y}_1^{m''}(\omega)[\mathcal{Y}_{l_1}^{m}(\omega)]^* \times e^{-\beta w_{\mathrm{LJ}}(r_{12})} \exp\left[-\sum_{m'=-1}^{1} u_{m'}(r_{12}) \mathcal{Y}_1^{m'}(\omega) \mathcal{Y}_1^{\overline{m'}}(\omega')\right] \mathcal{Y}_1^{\overline{m''}}(\omega')[\mathcal{Y}_{l_2}^{\overline{m}}(\omega')]^* \ . \tag{B10}$$

By expanding the product of two spherical harmonics of the same argument in a series of spherical harmonics [61], the right-hand side of Eq. (B10) can be expressed in terms of f itself [see Eq. (B8)] [69]:

$$\frac{\partial f_{l_1 l_2 m}(r_{12})}{\partial u_{m''}(r_{12})} = -\frac{3}{4\pi} \sum_{l_1', l_2'=0}^{\infty} \left[\frac{(2l_1+1)(2l_2+1)}{(2l_1'+1)(2l_2'+1)}\right]^{1/2} C(l_1 1 l_1', 000) C(l_1 1 l_1', \overline{m} m'' m') \times C(l_2 1 l_2', 000) C(l_2 1 l_2', m \overline{m}'' \overline{m}') f_{l_1' l_2' \overline{m'}}(r_{12}) \ , \tag{B11}$$

with $m' = \overline{m} + m''$ and $l_i + 1 + l_i' = \Delta$, $i \in \{1,2\}$.

In order to be able to exploit Eq. (B11) we have to determine the explicit dependence of $f_{000}(r_{12})$ on u_0, u_1, and u_{-1}. Then the other coefficients $f_{l_1 l_2 m}(r_{12})$ follow from employing Eq. (B11) in a recurrent manner. In most cases, due to the constraints $l_i + 1 + l_i' = \Delta$, for $i \in \{1,2\}$ the sum on the right-hand side reduces to a single term (e.g., for each $m \in \{-1,0,1\}$, $\partial f_{000}/\partial u_m$ is proportional to f_{11-m} only). If for a certain derivative on the left-hand side the sum on the right-hand side contains more than one term (e.g., $\partial f_{110}/\partial u_0$ is related to f_{000}, f_{200}, and f_{220}), one can always find another partial derivative leading to a different sum of the same coefficients $f_{l_1 l_2 m}$ (e.g., $\partial f_{111}/\partial u_1$ yields also terms with f_{000}, f_{200}, and f_{220}). By multiplying the corresponding equation with a suitable factor and then substracting it from the other one, a single coefficient $f_{l_1 l_2 m}$ can be isolated and determined (see below). Due to starting with f_{000} this procedure yields only those coefficients $f_{l_1 l_2 m}$ for which $l_1 + l_2$ is even. However, because $f_{l_1 l_2 m} = 0$ unless $l_1 + l_2$ is even [see (vi) in the preceding subsection], all nonvanishing coefficients $f_{l_1 l_2 m}(r_{12})$ can be derived from Eq. (B11). In this sense Eq. (B11) can be used as a recurrence formula.

3. The expansion coefficient of zeroth order for the Mayer function

In order to be able to use Eq. (B11) for determining the reduced expansion coefficients $f_{l_1 l_2 m}(r_{12})$, one must start by evaluating $f_{000}(r_{12})$, in particular as a function of the coefficients $u_{m'}(r_{12})$ entering Eq. (B8):

$$f_{000}(r_{12}) = -4\pi + \frac{1}{4\pi} e^{-\beta w_{\mathrm{LJ}}(r_{12})} \int_{S_2} d\omega \int_{S_2} d\omega' e^{-\sum_{m=-1}^{+1} u_m(r_{12}) \mathcal{Y}_1^m(\omega) \mathcal{Y}_1^{\overline{m}}(\omega')} = -4\pi + \frac{1}{4\pi} e^{-\beta w_{\mathrm{LJ}}(r_{12})} \mathcal{J}(\{u_m\}) \ . \tag{B12}$$

Note that the partial derivative on the left-hand side of Eq. (B11) tacitly assumes that the coefficients u_{-1}, u_0, and u_1 are independent from each other. Therefore Eq. (B12) must be calculated for arbitrary (real) coefficients u_m, which do *not* obey Eq. (B7). Once the differentiation is carried out, the corresponding expression is evaluated for the particular values for u_m given in Eq. (B7). Consequently, the argument of the exponential function in Eq. (B12) cannot be regarded to be real. Following Blum and Torruella [69], we rewrite this argument as a scalar product

$$\sum_{m=-1}^{+1} u_m(r_{12}) \mathcal{Y}_1^m(\omega) \mathcal{Y}_1^{\overline{m}}(\omega') = \mathbf{e}_1 \cdot \mathbf{A}, \tag{B13}$$

where the unit vector

$$\mathbf{e}_1 = \begin{bmatrix} \sin\theta_1 \cos\phi_1 \\ \sin\theta_1 \sin\phi_1 \\ \cos\theta_1 \end{bmatrix} \tag{B14}$$

denotes the direction of the first dipole moment and $\mathbf{A}$ is given by

$$\mathbf{A} = \frac{3}{4\pi} \begin{bmatrix} -\frac{1}{2}\sin\theta_2 (u_{-1} e^{i\phi_2} + u_1 e^{-i\phi_2}) \\ \frac{i}{2}\sin\theta_2 (u_{-1} e^{i\phi_2} - u_1 e^{-i\phi_2}) \\ u_0 \cos\theta_2 \end{bmatrix} = \mathbf{A}_1 + i\,\mathbf{A}_2 \ . \tag{B15}$$

The components of $\mathbf{e}_1$ and $\mathbf{A}$ correspond to a spatially fixed reference frame in which the intermolecular vector

$\mathbf{r}_{12}$ points into the z direction. $\mathbf{A}_1$ and $\mathbf{A}_2$ are real, with

$$\mathbf{A}_1=\frac{3}{4\pi}\begin{bmatrix}-\frac{1}{2}(u_{-1}+u_1)\sin\theta_2\cos\phi_2\\-\frac{1}{2}(u_{-1}+u_1)\sin\theta_2\sin\phi_2\\u_0\cos\theta_2\end{bmatrix} \tag{B16}$$

and

$$\mathbf{A}_2=\frac{3}{8\pi}(u_{-1}-u_1)\sin\theta_2\begin{bmatrix}-\sin\phi_2\\\cos\phi_2\\0\end{bmatrix} . \tag{B17}$$

Note that $\mathbf{A}_1$ and $\mathbf{A}_2$ are orthogonal for any value of u_{-1}, u_0, and u_1.

First we consider the function

$$f(\mathbf{A}_1,\mathbf{A}_2)=\int_{S_2}d\omega_1 e^{-\mathbf{e}_1\cdot\mathbf{A}_1-i\mathbf{e}_1\cdot\mathbf{A}_2} . \tag{B18}$$

Due to the properties of the scalar product for any rotation $\mathcal{D}$ in $\mathbb{R}^3$, the function f exhibits the following properties:

$$\begin{aligned}
&f(\mathcal{D}\mathbf{A}_1,\mathbf{A}_2)=f(\mathbf{A}_1,\mathcal{D}^{-1}\mathbf{A}_2) ,\\
&f(\mathbf{A}_1,\mathcal{D}\mathbf{A}_2)=f(\mathcal{D}^{-1}\mathbf{A}_1,\mathbf{A}_2) ,\\
&f(\mathcal{D}\mathbf{A}_1,\mathcal{D}\mathbf{A}_2)=f(\mathbf{A}_1,\mathbf{A}_2) ,\\
&f^*(\mathbf{A}_1,\mathbf{A}_2)=f(\mathbf{A}_1,-\mathbf{A}_2) ,\\
&f(\mathbf{A}_2,\mathbf{A}_1)=f\left(i\mathbf{A}_1,\frac{1}{i}\mathbf{A}_2\right) ,\\
&f(\mathbf{A}_1,\mathbf{A}_2)=H(\mathbf{A}_1+i\mathbf{A}_2) .
\end{aligned} \tag{B19}$$

These relations are fulfilled if f depends only on $\mathbf{A}^2$:

$$\begin{aligned}
f(\mathbf{A}_1,\mathbf{A}_2)&=g[(\mathbf{A}_1+i\mathbf{A}_2)^2]\\
&=g(v=\mathbf{A}_1\cdot\mathbf{A}_1-\mathbf{A}_2\cdot\mathbf{A}_2+2i\,\mathbf{A}_1\cdot\mathbf{A}_2) .
\end{aligned} \tag{B20}$$

This can be proven by expanding the integrand in Eq. (B18) in a Taylor series and by separately integrating its terms: $g(v)=4\pi[1+v^2/3+\mathcal{O}(v^4)]$. Thus one can rule out that $f(\mathbf{A}_1,\mathbf{A}_2)=\tilde{g}(|\mathbf{A}_1+i\mathbf{A}_2|^2)$ which would also be consistent with Eqs. (B19).

In the present case $\mathbf{A}_1\cdot\mathbf{A}_2=0$ so that the argument of g is real. Because $g^*(v)=g(v^*)$ [see Eqs. (B19)] it turns out that g is a real function of the real argument

$$\kappa=\mathbf{A}_1^2-\mathbf{A}_2^2=\left[\frac{3}{4\pi}\right]^2[u_1u_{-1}+(u_0^2-u_1u_{-1})\cos^2\theta_2] , \tag{B21}$$

which is independent of ϕ_2. This leads us to the following expression for the double integral $\mathcal{I}$ in Eq. (B12) as a function of the independent coefficients u_m:

$$\begin{aligned}
\mathcal{I}(\{u_m\})&=\int_0^{2\pi}d\phi_2\int_0^{\pi}d\theta_2\sin\theta_2\,g(\kappa)\\
&=4\pi\int_0^1 dx\,g\left[\left[\frac{3}{4\pi}\right]^2\right.\\
&\qquad\left.\times[u_1u_{-1}+(u_0^2-u_1u_{-1})x^2]\right] .
\end{aligned} \tag{B22}$$

Thus we are left with the determination of $g(\kappa)$.

Since κ is independent of ϕ_2, we can choose the particular value $\phi_2=0$. This results in [see Eqs. (B16) and (B17)]

$$g(\kappa)=\int_0^{2\pi}d\phi_1\int_0^{\pi}d\theta_1\sin\theta_1\exp\left[\frac{3}{8\pi}\sin\theta_2\sin\theta_1[(u_{-1}+u_1)\cos\phi_1-i(u_{-1}-u_1)\sin\phi_1]-\frac{3}{4\pi}u_0\cos\theta_2\cos\theta_1\right] . \tag{B23}$$

In the next step we evaluate Eq. (B23) for the particular value $\theta_2=0$. With $\kappa(\theta_2=0)=\kappa_0=(3/4\pi)^2u_0^2$ [see Eq. (B21)] one has

$$\begin{aligned}
g(\kappa_0)&=\int_0^{2\pi}d\phi_1\int_0^{\pi}d\theta_1\sin\theta_1 e^{-(3/4\pi)u_0\cos\theta_1}\\
&=2\pi\int_{-1}^{1}dx\,e^{-(\kappa_0)^{1/2}x}\\
&=\frac{2\pi}{\sqrt{\kappa_0}}[e^{(\kappa_0)^{1/2}}-e^{-(\kappa_0)^{1/2}}]\\
&=4\pi i_0(\sqrt{\kappa_0}) .
\end{aligned} \tag{B24}$$

Since $g(\kappa)$ depends on θ_2 only via the explicitly known θ_2 dependence of κ [see Eqs. (B20) and (B21)], we conclude that $g(\kappa)=4\pi i_0(\sqrt{\kappa})$. Note that even for negative values of κ, $g(\kappa)$ is real, because the series expansion of the modified spherical Bessel function of zero order $i_0(y)=(\sinh y)/y=\sum_{n=0}^{\infty}y^{2n}/(2n+1)!$ contains only terms of even powers of y. From Eqs. (B12), (B22), and (B24) we finally obtain

$$\begin{aligned}
&f_{000}(\{u_m(r_{12})\})\\
&\quad=-4\pi+2\pi e^{-\beta w_{\mathrm{LJ}}(r_{12})}\\
&\qquad\times\int_{-1}^{1}dx\,i_0\left[\frac{3}{4\pi}\mathcal{U}(\{u_m(r_{12})\},x)\right]
\end{aligned} \tag{B25}$$

with

$$\mathcal{U}(\{u_m\},x)=[u_{-1}u_1+(u_0^2-u_{-1}u_1)x^2]^{1/2} . \tag{B26}$$

Now $f_{000}(\{u_m(r_{12})\})$ has been cast into a form that can

be used in the recurrence relation given in Eq. (B11).

Furthermore, by inserting the particular values of u_m for the dipole interaction potential [see Eq. (B7)] one obtains from Eq. (B3) the lowest-order expansion coefficient of the Mayer function in the spatially fixed reference frame:

$$\hat{f}_{000}(r_{12})=(4\pi)^{3/2}\left[-1+e^{-\beta w_{\mathrm{LJ}}(r_{12})}\int_0^1 dx\, i_0[\mathcal{Z}h(x)]\right], \tag{B27}$$

where $\mathcal{Z}=\beta m^2/r_{12}^3$ (see Sec. III A) and $h(x)=(1+3x^2)^{1/2}$. Note that Eq. (B27) is consistent with Eq. (3.9).

Due to the above-mentioned series expansion of i_0, one can easily verify the asymptotic behavior $\hat{f}_{000}(r_{12}\to\infty)\sim r_{12}^{-6}$ by separately integrating each term of the expansion. Concerning the parameters β and m, one has $\hat{f}_{000}(\beta\to 0,m,r_{12})\sim\beta^2$ as well as $\hat{f}_{000}(\beta,m\to 0,r_{12})\sim m^4$.

4. The expansion coefficients of first order for the Mayer function

The first-order reduced coefficients $f_{11m}(r_{12})$ can be derived from the zeroth-order coefficient [Eq. (B25)] by using the recurrence relation in Eq. (B11). There the constraint $|m'|\le\min(l_1',l_2')$ for the Clebsch-Gordan coefficients reduces the sum on the right-hand side of Eq. (B11) to a single term for each partial derivative of f_{000} with respect to u_0, u_{-1}, and u_1, respectively. One obtains

$$f_{110}(r_{12})=-4\pi\frac{\partial f_{000}(r_{12})}{\partial u_0(r_{12})}=-12\pi e^{-\beta w_{\mathrm{LJ}}(r_{12})}\int_0^1 dx\frac{i_1\left[\frac{3}{4\pi}\mathcal{U}(\{u_m\},x)\right]x^2u_0}{\mathcal{U}(\{u_m\},x)}, \tag{B28}$$

$$f_{111}(r_{12})=-4\pi\frac{\partial f_{000}(r_{12})}{\partial u_{-1}(r_{12})}=-6\pi e^{-\beta w_{\mathrm{LJ}}(r_{12})}\int_0^1 dx\frac{i_1\left[\frac{3}{4\pi}\mathcal{U}(\{u_m\},x)\right](1-x^2)u_1}{\mathcal{U}(\{u_m\},x)}, \tag{B29}$$

$$f_{11-1}(r_{12})=-4\pi\frac{\partial f_{000}(r_{12})}{\partial u_1(r_{12})}=-6\pi e^{-\beta w_{\mathrm{LJ}}(r_{12})}\int_0^1 dx\frac{i_1\left[\frac{3}{4\pi}\mathcal{U}(\{u_m\},x)\right](1-x^2)u_{-1}}{\mathcal{U}(\{u_m\},x)}, \tag{B30}$$

where $\mathcal{U}(\{u_m\},x)$ is defined by Eq. (B26) and $i_1(y)=[di_0(y)]/dy=(\cosh y)/y-(\sinh y)/y^2$ is the modified spherical Bessel function of first order. Using Eq. (B3) one derives the coefficients $\hat{f}_\Lambda$ of first order in the spatially fixed frame of reference as

$$\hat{f}_{110}(r_{12})=6\pi\left[\frac{4\pi}{3}\right]^{1/2}e^{-\beta w_{\mathrm{LJ}}(r_{12})}\times\int_0^1 dx\frac{2u_0x^2-(u_{-1}+u_1)(1-x^2)}{\mathcal{U}(\{u_m\},x)}\times i_1\left[\frac{3}{4\pi}\mathcal{U}(\{u_m\},x)\right], \tag{B31}$$

$$\hat{f}_{112}(r_{12})=2\pi\left[\frac{6\pi}{5}\right]^{1/2}e^{-\beta w_{\mathrm{LJ}}(r_{12})}\times\int_0^1 dx\frac{4u_0x^2+(u_{-1}+u_1)(1-x^2)}{\mathcal{U}(\{u_m\},x)}\times i_1\left[\frac{3}{4\pi}\mathcal{U}(\{u_m\},x)\right]. \tag{B32}$$

In the particular case where the anisotropic part of the intermolecular interaction is the dipole-dipole potential, one has to insert the values for u_m given by Eq. (B7):

$$\hat{f}_{110}(r_{12})=12\pi\left[\frac{4\pi}{3}\right]^{1/2}e^{-\beta w_{\mathrm{LJ}}(r_{12})}\times\int_0^1 dx\frac{1-3x^2}{h(x)}i_1(\mathcal{Z}h(x)), \tag{B33}$$

$$\hat{f}_{112}(r_{12})=12\pi\left[\frac{2\pi}{15}\right]^{1/2}e^{-\beta w_{\mathrm{LJ}}(r_{12})}\times\int_0^1 dx\frac{1+3x^2}{h(x)}i_1(\mathcal{Z}h(x)). \tag{B34}$$

Their asymptotic behavior for $\mathcal{Z}\to 0$ (which is equivalent to $\beta\to 0$, $m\to 0$, or $r_{12}\to\infty$) can be inferred from integrating each term of the series expansion of $i_1(\mathcal{Z}h(x))$. Due to

$$i_1(y)=\sum_{n=1}^{\infty}\left[\frac{1}{(2n)!}-\frac{1}{(2n+1)!}\right]y^{2n-1},$$

one obtains $\hat{f}_{11l}(\mathcal{Z}\to 0)\sim\mathcal{Z}$, for $l\in\{0,2\}$ or, in terms of the intermolecular distance, $\hat{f}_{11l}(r_{12}\to\infty)\sim r_{12}^{-3}$, for $l\in\{0,2\}$, respectively.

5. The expansion coefficients of second order for the Mayer function

In the absence of symmetry-breaking external fields, the first-order expansion coefficients $\hat{f}_{110}$ and $\hat{f}_{112}$ do not enter Eq. (4.27) (see Sec. IV B). However, the reduced coefficients $f_{11m}(\{u_m\})$ are needed to obtain the second-order expansion coefficients, which do enter Eq. (4.27). They follow from taking the partial derivatives of f_{11m} with respect to $u_{m'}$, where the indices $m,m' \in \{-1,0,1\}$. Due to the aforementioned constraints of the Clebsch-Gordan coefficients, again, in some cases, the sum on the right-hand side of Eq. (B11) reduces to a single term. This leads to

$$f_{221}(r_{12}) = -\frac{20\pi}{3}\frac{\partial f_{110}(r_{12})}{\partial u_{-1}(r_{12})} = 30\pi e^{-\beta w_{\mathrm{LJ}}(r_{12})} \times \int_0^1 dx \frac{\overline{T}(\mathcal{U}(\{u_m\},x))}{\mathcal{U}^2(\{u_m\},x)} u_0 u_1 x^2(1-x^2) , \tag{B35}$$

$$f_{22-1}(r_{12}) = -\frac{20\pi}{3}\frac{\partial f_{110}(r_{12})}{\partial u_1(r_{12})} = 30\pi e^{-\beta w_{\mathrm{LJ}}(r_{12})} \times \int_0^1 dx \frac{\overline{T}(\mathcal{U}(\{u_m\},x))}{\mathcal{U}^2(\{u_m\},x)} u_0 u_{-1} x^2(1-x^2) , \tag{B36}$$

$$f_{222}(r_{12}) = -\frac{20\pi}{6}\frac{\partial f_{111}(r_{12})}{\partial u_{-1}(r_{12})} = \frac{15\pi}{2} e^{-\beta w_{\mathrm{LJ}}(r_{12})} \times \int_0^1 dx \frac{\overline{T}(\mathcal{U}(\{u_m\},x))}{\mathcal{U}^2(\{u_m\},x)} u_1^2(1-x^2)^2 , \tag{B37}$$

$$f_{22-2}(r_{12}) = -\frac{20\pi}{6}\frac{\partial f_{11-1}(r_{12})}{\partial u_1(r_{12})} = \frac{15\pi}{2} e^{-\beta w_{\mathrm{LJ}}(r_{12})} \times \int_0^1 dx \frac{\overline{T}(\mathcal{U}(\{u_m\},x))}{\mathcal{U}^2(\{u_m\},x)} u_{-1}^2(1-x^2)^2 , \tag{B38}$$

where we have introduced the function

$$\overline{T}(\mathcal{U}(\{u_m\},x)) = i_0\left[\frac{3}{4\pi}\mathcal{U}(\{u_m\},x)\right] - \frac{3}{\frac{3}{4\pi}\mathcal{U}(\{u_m\},x)} i_1\left[\frac{3}{4\pi}\mathcal{U}(\{u_m\},x)\right] . \tag{B39}$$

The remaining coefficients f_{200} and f_{220} follow from

$$\frac{\partial f_{110}(r_{12})}{\partial u_0(r_{12})} = -\frac{1}{4\pi}\left[f_{000}(r_{12}) + \frac{4}{\sqrt{5}} f_{200}(r_{12}) + \tfrac{4}{5} f_{220}(r_{12})\right] \tag{B40}$$

and

$$\frac{\partial f_{111}(r_{12})}{\partial u_1(r_{12})} = -\frac{1}{4\pi}\left[f_{000}(r_{12}) - \frac{2}{\sqrt{5}} f_{200}(r_{12}) + \tfrac{1}{5} f_{220}(r_{12})\right] , \tag{B41}$$

so that one obtains

$$f_{220}(r_{12}) = -\frac{5}{2}\left[f_{000}(r_{12}) + \frac{4\pi}{3}\left[\frac{\partial f_{110}(r_{12})}{\partial u_0(r_{12})} + \frac{\partial f_{111}(r_{12})}{\partial u_1(r_{12})}\right]\right] = 5\pi e^{-\beta w_{\mathrm{LJ}}(r_{12})} \int_0^1 dx \frac{\overline{T}(\mathcal{U}(\{u_m\},x))}{\mathcal{U}^2(\{u_m\},x)} [3x^4(2u_0^2 + u_1 u_{-1}) - 2x^2(u_0^2 + 2u_1 u_{-1}) + u_1 u_{-1}] . \tag{B42}$$

The insertion of Eq. (B42) into Eq. (B40) yields the following expression for f_{200}:

$$f_{200}(r_{12}) = -\frac{\sqrt{5}}{4}\left[f_{000} + 4\pi\frac{\partial f_{110}(r_{12})}{\partial u_0(r_{12})} + \tfrac{4}{5} f_{220}(r_{12})\right] = \sqrt{5}\pi e^{-\beta w_{\mathrm{LJ}}(r_{12})} \int_0^1 dx \left\{\frac{\overline{T}(\mathcal{U}(\{u_m\},x))}{\mathcal{U}^2(\{u_m\},x)} [3x^4(u_0^2 - u_1 u_{-1}) + 2x^2(u_0^2 + 2u_1 u_{-1}) - u_1 u_{-1}] - \left[i_0\left[\frac{3}{4\pi}\mathcal{U}(\{u_m\},x)\right] - 3x^2\frac{3}{\frac{3}{4\pi}\mathcal{U}(\{u_m\},x)} i_1\left[\frac{3}{4\pi}\mathcal{U}(\{u_m\},x)\right]\right]\right\} . \tag{B43}$$

As in the previous subsections Eq. (B3) allows us to obtain the coefficients $\hat{f}_\Lambda$ in the spatially fixed reference frame:

$$\hat{f}_{202}(r_{12})=2\pi\sqrt{\pi}e^{-\beta w_{\mathrm{LJ}}(r_{12})}\int_0^1 dx\left\{\frac{\overline{\mathcal{T}}(U(\{u_m\},x))}{\mathcal{U}^2(\{u_m\},x)}[3x^4(u_0^2-u_1u_{-1})+2x^2(u_0^2+2u_1u_{-1})-u_1u_{-1}]\right.$$
$$\left.-\left[i_0\left[\frac{3}{4\pi}\mathcal{U}(\{u_m\},x)\right]-3x^2\frac{3}{\frac{3}{4\pi}\mathcal{U}(\{u_m\},x)}i_1\left[\frac{3}{4\pi}\mathcal{U}(\{u_m\},x)\right]\right]\right\}, \quad \text{(B44)}$$

$$\hat{f}_{220}(r_{12})=2\pi\sqrt{5\pi}e^{-\beta w_{\mathrm{LJ}}(r_{12})}$$
$$\times\int_0^1 dx\frac{\overline{\mathcal{T}}(\mathcal{U}(\{u_m\},x))}{\mathcal{U}^2(\{u_m\},x)}\{\tfrac{3}{2}x^4[4u_0^2+u_1^2+u_{-1}^2+4u_0(u_1+u_{-1})+2u_1u_{-1}]$$
$$-x^2[2u_0^2+3(u_1^2+u_{-1}^2)+6u_0(u_1+u_{-1})+4u_1u_{-1}]$$
$$+\tfrac{1}{2}[3(u_1^2+u_{-1}^2)+2u_1u_{-1}]\}, \quad \text{(B45)}$$

$$\hat{f}_{222}(r_{12})=2\pi\left[\frac{5\pi}{14}\right]^{1/2}e^{-\beta w_{\mathrm{LJ}}(r_{12})}\int_0^1 dx\frac{\overline{\mathcal{T}}(\mathcal{U}(\{u_m\},x))}{\mathcal{U}^2(\{u_m\},x)}\{3x^4[-4u_0^2+u_1^2+u_{-1}^2-2u_0(u_1+u_{-1})-2u_1u_{-1}]$$
$$-2x^2[2u_0^2-3(u_1^2+u_{-1}^2)+3u_0(u_1+u_{-1})+4u_1u_{-1}]$$
$$+[3(u_1^2+u_{-1}^2)-2u_1u_{-1}]\}, \quad \text{(B46)}$$

$$\hat{f}_{224}(r_{12})=5\pi\left[\frac{\pi}{70}\right]^{1/2}e^{-\beta w_{\mathrm{LJ}}(r_{12})}\int_0^1 dx\frac{\overline{\mathcal{T}}(\mathcal{U}(\{u_m\},x))}{\mathcal{U}^2(\{u_m\},x)}\{x^4[24u_0^2+u_1^2+u_{-1}^2-16u_0(u_1+u_{-1})+12u_1u_{-1}]$$
$$+2x^2[-4u_0^2-(u_1^2+u_{-1}^2)+8u_0(u_1+u_{-1})-8u_1u_{-1}]$$
$$+(u_1^2+u_{-1}^2+4u_1u_{-1})\}. \quad \text{(B47)}$$

Finally, Eqs. (B44)–(B47) are evaluated for those values of u_0, u_{-1}, and u_1, which correspond to the dipole-dipole interaction potential [see Eq. (B7)]:

$$\hat{f}_{022}(r_{12})=\hat{f}_{202}(r_{12})=2\pi\sqrt{\pi}e^{-\beta w_{\mathrm{LJ}}(r_{12})}\left[\int_0^1 dx\frac{9x^4+12x^2-1}{1+3x^2}\mathcal{T}(\mathcal{Z}h(x))\right.$$
$$\left.-\int_0^1 dx\left[i_0(\mathcal{Z}h(x))-3x^2\frac{3}{\mathcal{Z}h(x)}i_1(\mathcal{Z}h(x))\right]\right], \quad \text{(B48)}$$

$$\hat{f}_{220}(r_{12})=4\pi\sqrt{\pi}\sqrt{5}e^{-\beta w_{\mathrm{LJ}}(r_{12})}\int_0^1 dx\frac{27x^4-21x^2+2}{1+3x^2}\mathcal{T}(\mathcal{Z}h(x)), \quad \text{(B49)}$$

$$\hat{f}_{222}(r_{12})=4\pi\left[\frac{10\pi}{7}\right]^{1/2}e^{-\beta w_{\mathrm{LJ}}(r_{12})}\int_0^1 dx\frac{-18x^4+9x^2+1}{1+3x^2}\mathcal{T}(\mathcal{Z}h(x)), \quad \text{(B50)}$$

$$\hat{f}_{224}(r_{12})=10\pi\left[\frac{\pi}{70}\right]^{1/2}e^{-\beta w_{\mathrm{LJ}}(r_{12})}\int_0^1 dx\frac{23x^4+6x^2+3}{1+3x^2}\mathcal{T}(\mathcal{Z}h(x)). \quad \text{(B51)}$$

The function $\mathcal{T}(y)=i_0(y)-(3/y)i_1(y)$ determines the asymptotic behavior of the second-order coefficients for large distances. Due to its series expansion

$$\mathcal{T}(y)=\sum_{n=0}^{\infty}\left[\frac{1}{(2n+1)!}-\frac{3}{(2n+2)!}+\frac{3}{(2n+3)!}\right]y^{2n} \quad \text{(B52)}$$

one can infer, by separately integrating each term of the series, that $\hat{f}_{l_1l_2l}(\mathcal{Z}\to 0)\sim\mathcal{Z}^2$, or, in terms of the intermolecular distance, $\hat{f}_{l_1l_2l}(r_{12}\to\infty)\sim r_{12}^{-6}$. This holds for every second-order coefficient, i.e., for $(l_1l_2l)\in\{(202),(022),(220),(222),(224)\}$.

APPENDIX C: EXPANSION COEFFICIENTS OF THE MAYER FUNCTION FOR NEMATIC LIQUIDS

For $w_{\mathrm{ex}}(\mathbf{r},\mathbf{r},\omega,\omega')=w_{\mathrm{nem}}(r_{12},\omega,\omega',\omega_{12})$ given in Eq. (5.2), the same procedure can be carried out as in Appen-

dix B for the dipole-dipole interaction potential. Following Eq. (B5), one expands $\beta\tilde{w}_{\rm nem}$, where $\tilde{w}_{\rm nem}=w_{\rm nem}+A(\sigma/r_{12})^6$ is the anisotropic part of $w_{\rm nem}$, in terms of the rotational invariants $\Phi_\Lambda(\omega,\omega',\omega_{12})$:

$$\beta\tilde{w}_{\rm nem}(r_{12},\omega,\omega',\omega_{12})=\sum_\Lambda \hat{u}^{\rm nem}_\Lambda(r_{12})\Phi_\Lambda(\omega,\omega',\omega_{12}) , \quad \text{(C1)}$$

with $\Lambda=(l_1l_2l)\in\{(022),(202),(220)\}$ and [see Eq. (5.2)]

$$\hat{u}^{\rm nem}_{220}(r_{12})=-\beta B(4\pi)^{3/2}\frac{1}{\sqrt{5}}\left[\frac{\sigma}{r_{12}}\right]^6 \quad \text{(C2)}$$

and

$$\hat{u}^{\rm nem}_{202}(r_{12})=\hat{u}^{\rm nem}_{022}(r_{12})=\beta C(4\pi)^{3/2}\tfrac{1}{5}\left[\frac{\sigma}{r_{12}}\right]^6 . \quad \text{(C3)}$$

Thus for nematic liquids there are seven reduced coefficients $u^{\rm nem}_{l_1l_2m}(r_{12})$ [compare Eqs. (B2) and (4.16)] and (B5): $(l_1l_2m)\in\{(020),(200),(220),(22\pm1),(22\pm2)\}=\mathbb{L}$. Inserting this into the adequately generalized versions of Eqs. (B8) and (B10) yields the analogue of the recurrence relation in Eq. (B11). Then the same algebraic operations are carried out as in Appendix B 4 and B 5 provided one has determined the explicit expression of the zeroth-order expansion coefficient for the Mayer function

$$f^{\rm nem}_{000}(r_{12})=-4\pi+\frac{1}{4\pi}e^{-\beta A(\sigma/r_{12})^6}\int_{S_2}d\omega\int_{S_2}d\omega'\exp\left[-\sum_{(l_1,l_2,m)\in\mathbb{L}}u^{\rm nem}_{l_1l_2m}(r_{12})\mathcal{Y}^m_{l_1}(\omega)\mathcal{Y}^{\bar{m}}_{l_2}(\omega')\right] \quad \text{(C4)}$$

for arbitrary $u^{\rm nem}_{l_1l_2m}$.

[1] J. P. Hansen and I. A. McDonald, *Theory of Simple Liquids* (Academic, London, 1986).
[2] H. Frisch and J. L. Lebowitz, *The Equilibrium Theory of Classical Fluids* (Benjamin, New York, 1964).
[3] *Fluid Interfacial Phenomena,* edited by C. A. Croxton (Wiley, Chichester, 1986).
[4] J. K. Percus and G. O. Williams, in *Fluid Interfacial Phenomena* (Ref. [3]), p. 1.
[5] P. G. de Gennes, Rev. Mod. Phys. **57**, 827 (1985).
[6] D. E. Sullivan and M. M. Telo da Gama, in *Fluid Interfacial Phenomena* (Ref. [3]), p. 45.
[7] S. Dietrich, in *Phase Transitions and Critical Phenomena,* edited by C. Domb and J. L. Lebowitz (Academic, London, 1988), Vol. 12, p. 1.
[8] *Liquids at Interfaces,* edited by J. Charvolin, J. F. Joanny, and J. Zinn-Justin, Les Houches Summer School Lectures, Session XLVIII (Elsevier, Amsterdam, 1990); see in particular the contributions by P. Evans, P. G. de Gennes, J. Meunier, A. M. Cazabat, M. Schick, and D. Beysens.
[9] R. Evans, J. Phys. Condens. Matter **2**, 8989 (1990).
[10] J. O. Indekeu, *Topics in Wetting Phenomena,* Habilitation thesis, Katholieke Universiteit Leuven, 1991 (unpublished).
[11] G. Forgács, T. Nieuwenhuizen, and R. Lipowsky, in *Phase Transitions and Critical Phenomena,* Vol. 14, edited by C. Domb and J. L. Lewobitz (Academic, London, in press).
[12] R. Evans, Adv. Phys. **28**, 143 (1979).
[13] S. Dietrich and M. Napiórkowski, Phys. Rev. A **43**, 1861 (1991).
[14] P. I. Teixeria and M. M. Telo da Gama, J. Phys. Condens. Matter **3**, 111 (1991).
[15] A. Poniewierski and R. Holyst, Phys. Rev. Lett. **61**, 2461 (1988); Phys. Rev. A **41**, 6871 (1990).
[16] See T. J. Sluckin and A. Poniewierski, in *Fluid Interfacial Phenomena* (Ref. [3]), p. 215; B. Jérôme, Rep. Prog. Phys. **54**, 391 (1991), and references cited therein.
[17] P. Sheng, Phys. Rev. Lett. **37**, 1059 (1976); Phys. Rev. A **26**, 1610 (1982); A. K. Sen and D. E. Sullivan, *ibid.* **35**, 1391 (1986).
[18] M. M. Telo da Gama, Mol. Phys. **52**, 585 (1984); **52**, 611 (1984); J. V. Seliger and D. R. Nelson, Phys. Rev. A **37**, 1736 (1988).
[19] J. H. Thurtell, M. M. Telo da Gama, and K. E. Gubbins, Mol. Phys. **54**, 321 (1985); B. Tjipto-Margo, A. K. Sen, L. Mederos, and D. E. Sullivan, *ibid.* **67**, 601 (1989).
[20] W. H. Keesom, Phys. Z. **22**, 129 (1921).
[21] L. Onsager, Chem. Rev. **13**, 73 (1933).
[22] G. S. Rushbroke, Trans. Faraday Soc. **36**, 1055 (1940).
[23] D. Cook and J. S. Rowlinson, Proc. R. Soc. London, Ser. A **219**, 405 (1949).
[24] C. E. Woodward and S. Nordholm, Mol. Phys. **52**, 973 (1984); **59**, 1177 (1986).
[25] G. Stell, Phys. Rev. Lett. **32**, 286 (1974).
[26] D. Y. C. Chan and G. R. Walker, Mol. Phys. **47**, 881 (1982).
[27] P. H. Fries and G. N. Patey, J. Chem. Phys. **82**, 429 (1985); A. Perera, P. G. Kusalik, and G. N. Patey, *ibid.* **87**, 1295 (1987); **89**, 5969 (1988); A. Perera and G. N. Patey, *ibid.* **89**, 5861 (1988).
[28] E. Lomba, M. Lombardero, and J. L. F. Abascal, J. Chem. Phys. **91**, 2581 (1989).
[29] P. G. Kusalik, Mol. Phys. **67**, 67 (1989).
[30] A. Perera and G. N. Patey, J. Chem. Phys. **91**, 3045 (1989).
[31] A. Perera, G. N. Patey, and J. J. Weis, J. Chem. Phys. **89**, 6941 (1988).
[32] V. Russier, J. Chem. Phys. **90**, 4491 (1989).
[33] G. M. Torrie, A. Perera, and G. N. Patey, Mol. Phys. **67**, 1337 (1989).
[34] J. P. Badiali, J. Phys. Chem. **89**, 2397 (1988); J. Chem. Phys. **90**, 4401 (1989); J. P. Badiali and F. Forstmann, Chem. Phys. **141**, 63 (1990); Q. Zhang, J. P. Badiali, and W. H. Su, J. Chem. Phys. **92**, 4609 (1990).

[35] C. E. Woodward and S. Nordholm, Mol. Phys. **60**, 415 (1987).
[36] M. Moradi and G. Rickayzen, Mol. Phys. **68**, 903 (1989).
[37] See L. Blum, in *Fluid Interfacial Phenomena* (Ref. [3]), p. 391.
[38] See K. E. Gubbins, in *Fluid Interfacial Phenomena* (Ref. [3]), p. 469.
[39] J. M. Haile, C. G. Gray, and K. E. Gubbins, J. Chem. Phys. **64**, 2569 (1976).
[40] J. M. Haile, K. E. Gubbins, and C. G. Gray, J. Chem. Phys. **64**, 1852 (1976).
[41] S. M. Thompson and K. E. Gubbins, J. Chem. Phys. **70**, 4947 (1979).
[42] See Secs. 2.6 and 2.7 in C. G. Gray and K. E. Gubbins, *Theory of Molecular Fluids* (Clarendon, Oxford, 1984).
[43] S. M. Thompson, K. E. Gubbins, and J. M. Haile, J. Chem. Phys. **75**, 1325 (1981).
[44] P. Tarazona and G. Navascués, Mol. Phys. **47**, 145 (1982).
[45] E. Chacón, P. Tarazona, and G. Navascués, J. Chem. Phys. **79**, 4426 (1983); Mol. Phys. **51**, 1475 (1984).
[46] J. Eggebrecht, K. E. Gubbins, and S. M. Thompson, J. Chem. Phys. **86**, 2286 (1987).
[47] J. Eggebrecht, S. M. Thompson, and K. E. Gubbins, J. Chem. Phys. **86**, 2299 (1987).
[48] R. Evans, P. Tarazona, and U. Marini Bettolo Marconi, Mol. Phys. **50**, 993 (1983).
[49] S. Dietrich, M. P. Nightingale, and M. Schick, Phys. Rev. B **32**, 3182 (1985).
[50] J. A. Barker and D. Henderson, J. Chem. Phys. **47**, 2856 (1967).
[51] We note that it is possible to choose other reference systems, e.g., those formed by nonspherical molecules, in order to construct more realistic models of dipolar fluids. In this paper, however, we restrict ourselves to hard spheres.
[52] N. F. Carnahan and K. E. Starling, J. Chem. Phys. **51**, 635 (1969).
[53] J. A. Barker and D. Henderson, J. Chem. Phys. **47**, 4714 (1967).
[54] P. Palffy-Muhoray, M. A. Lee, and R. G. Petschek, Phys. Rev. Lett. **60**, 2303 (1988).
[55] J. M. Mercer, Mol. Phys. **69**, 625 (1990).
[56] $i_n(x)$ is a convenient notation for the modified spherical Bessel functions $\sqrt{\pi/2z}\,I_{n+1/2}(z)$ using the notation of *Handbook of Mathematical Functions,* edited by M. Abramowitz and I. A. Stegun (Dover, New York, 1970), Eq. (10.2.12).
[57] The same effective pair potential has been discussed by Woodward and Nordholm (see Ref. [24]). However, one of their series representations for the angular average of the exponential of the dipole-dipole potential [Eq. (14) in Mol. Phys. **52**, 973 (1984)] is incorrect.
[58] J.-P. Hansen and L. Verlet, Phys. Rev. **184**, 151 (1969).
[59] A. Z. Panagiotopoulos, Mol. Phys. **61**, 813 (1987).
[60] B. Smit, C. P. Williams, E. M. Hendriks, and S. W. De Leeuw, Mol. Phys. **68**, 765 (1989).
[61] For details see Sec. 2.3 and Appendix A in Ref. [42].
[62] M. E. Rose, *Elementary Theory of Angular Momentum* (Wiley, New York, 1957).
[63] S. Dietrich and M. Schick, Phys. Rev. B **33**, 4952 (1986).
[64] M. Napiórkowski and S. Dietrich, Europhys. Lett. **9**, 361 (1989).
[65] See P. G. de Gennes, *The Physics of Liquid Crystals* (Clarendon, Oxford, 1974), and D. Frenkel, in *Liquids, Freezing and Glass Transition,* edited by J. P. Hansen, D. Levesque, and J. Zinn-Justin, Les Houches, Session LI, 1989 (Elsevier, Amsterdam, 1991), p. 691.
[66] L. Onsager, Ann. N.Y. Acad. Sci. **51**, 627 (1949).
[67] R. Hołyst and A. Poniewierski, Mol. Phys. **65**, 1081 (1988).
[68] B. G. Moore and W. E. McMullen, Phys. Rev. A **42**, 6042 (1990).
[69] L. Blum and A. J. Torruella, J. Chem. Phys. **89**, 4976 (1988).